5-2016

EXAMINATION OF CD133 AND CD147 AS CANCER STEM CELL MARKERS

Christopher McMahon
cmcmahon@nmu.edu

EXAMINATION OF CD133 AND CD147 AS CANCER STEM CELL MARKERS

By

Christopher McMahon

THESIS

Submitted to
Northern Michigan University
In partial fulfillment of the requirements
For the degree of

MASTER OF SCIENCE

Office of Graduate Education and Research

May 2016

SIGNATURE APPROVAL FORM

Title of Thesis: EXAMINATION OF CD133 AND CD147 AS CANCER STEM CELL MARKERS

This thesis by Christopher McMahon is recommended for approval by the student's Thesis Committee and Department Head in the NMU Department of Biology and by the Assistant Provost of Graduate Education and Research

_____

Committee Chair: Robert Winn, PhD Date

_____

First Reader: Johnathan Lawrence, PhD Date

_____

Second Reader: Robert Belton, PhD Date

_____

Department Head: John Rebers, PhD Date

_____

Robert Winn, PhD Date

Interim Assistant Provost of Graduate Education and Research

ABSTRACT

EXAMINATION OF CD133 AND CD147 AS CANCER STEM CELL MARKERS

By

Christopher McMahon

To date, as many as 14,000 patients in the United States per year are diagnosed with glioblastoma, the most common and most malignant primary brain tumor. Glioblastomas are characterized by their ability to evade treatment on many fronts, thus a novel approach to curative therapies is imperative. A population of cells with stem cell-like properties are found within glioblastoma tumors and drive their initiation and progression. Identification of extracellular markers on these tumor stem cells is thus paramount. The cell surface glycoproteins CD133 and CD147 were examined as potential markers of cancer stem cells found in glioblastoma. Here we found evidence which shows that formation of neurospheres with U87MG glioblastoma cells may be driven by increased expression of CD147, correlated with increased CD133 expression. These findings suggest that relative levels of CD147 expression may be used as a determinant to target cancer stem cells in glioblastoma.

DEDICATION

For Steph and Maddie.

ACKNOWLEDGEMENTS

I foremost wish to thank Dr. Rob Winn, my adviser and mentor as both undergraduate and graduate, who taught me how to learn, how to teach, how to do research, and to make sure I hit it past the women's tee box. Without him, completion of this degree was impossible. Secondly, I owe considerable thanks to Dr. John Lawrence who guided me through most every step of the project, from conception to completion, and carried me through the others. Thanks also to Dr. Robert Belton, who always punctuates criticism with a smile.

I would be remiss if I also didn't mention Dr. Erich Ottem for his help with the confocal microscope; Samantha Wightman for helping me get back on the horse; Aaron Mellesmoen who always had stem cells when I needed them; Bridget Waas, Melanie Flaherty, and Amanda Wigand for all the little things; Dr. Paul Mann for his qPCR help and use of his facilities and equipment; and Dr. Richard Rovin, whom helped get it all started.

This thesis follows the format prescribed by the CBE Style Manual and the NMU Department of Biology.

TABLE OF CONTENTS

LIST OF FIGURES

LIST OF ABBREVIATIONS

AMV-RT – Avian myeloblastosis virus - reverse transcriptase

Bp – Base pair

bFGF – Basic fibroblast growth factor

BSA – Bovine serum albumin

cDNA – Complimentary deoxyribonucleic acid

CRISPR – Clustered regularly interspaced short palindromic repeats

CSC – Cancer stem cell

CT – Cycle threshold

DAPI - 4′,6-diamidino-2-phenylindole

DMEM – Dulbecco's Modified Eagle's Medium

DMSO – Dimethyl sulfoxide

DNA – Deoxyribonucleic acid

dNTP – Reagent mixture of deoxyribonucleotides: dATP, dCTP, dGTP, dTTP

EDTA – Ethylene diamine triacetic acid

EGF – Epidermal growth factor

EMEM – Eagle's Modified Essential Medium

FACS – Fluorescence-activated cell sorting

FBS – Fetal bovine serum

FITC – Fluorescein isothiocyanate

GBM – Glioblastoma multiforme

HEPES – 4-(2-hydroxyethyl)-1-piperazineethane sulfonic acid

MCT – Monocarboxylate transporter

MMP – Matrix metalloproteinase

MGMT – O6-methylguanine-DNA-methyltransferase

mRNA – Messenger RNA

MW – Molecular weight

PBS – Phosphate-buffered saline

PCR – Polymerase chain-reaction

PSA – Penicillin-Streptomycin-Amphotericin B

qPCR – Quantitative PCR

RNA – Ribonucleic acid

RT – Room temperature

TMZ – Temozolomide

VEGF – Vascular endothelial growth factor

WHO – World Health Organization

INTRODUCTION

Glioblastoma (GBM) is the most prevalent central nervous system-borne primary brain tumor found in adults. They are typically exceedingly aggressive tumors; 90% of patients die within three years and half fail to see a second year[1]. What is equally problematic is that they are also exceedingly difficult to treat. Surgery, and modern chemotherapy and radiotherapy are largely unsuccessful. Patients are also largely at risk for recurrent tumors[2].

What is currently highly regarded as the theory behind GBM tumors' resistance to treatment is the cancer stem cell theory. This theory proposes that within a GBM tumor there are different tumorigenic phenotypes; one of these phenotypically-different cells is capable, if transplanted into a host, of generating new tumors. This type of cell is referred to as a cancer stem cell (CSC) because of its similarity to normal stem cells[3]. The CSC theory postulates that this small subpopulation of cancer cells drives tumor growth; of any given GBM tumor, only 1-30% of the total cell volume is comprised of CSCs[4]. As they exhibit characteristics of normal stem cells, they are potentially able to differentiate into neuronal, astroglial, and oligodendroglial cells; the resulting tumor will characteristically be a mixture of cell types[2-3].

The majority of primary neurological tumors in adults are glial-cell derived, and of those, GBM are the most prevalent. Despite their prevalence, there are few treatment options. This is due largely to a multifaceted approach of GBMs to thwart attempts to combat it. GBM tumor cells alter adjacent normal cells to facilitate growth of tumor

cells, invasion, resistance to chemical treatment, evasion of immune attack, and metastasis[1-3]. And while the human immune system can typically initially retard tumor growth, it is often thwarted by immunosuppressive pathways activated by tumor cells[3].

It has also been shown that non-CSCs may have the ability to revert back to CSCs under particular environmental cues[5]; CSC traits may be acquired via the epithelial to mesenchymal transition (EMT). Through this process, (differentiated) epithelial cells can assume the mesenchymal phenotype, to wit: the ability to migrate, invade, and resist apoptosis[6]. Thus, even benign tumor cells may eventually exhibit invasiveness and metastatic potential. It seems then that GBM cells may simply be classified into CSCs and "not-as-yet CSCs". Therefore, removing even 99% of the mass of a typical GBM tumor and subsequently treating the remaining mass of cells with chemo- and radiotherapy is scarcely a guarantee of success; the <1% that remains could certainly possess the ability to regrow the tumor, metastasize, etc. It is thus paramount that we be able to identify and target what is constitutively a CSC.

LITERATURE REVIEW

CD133

GBMs, or Grade IV astrocytomas, are highly proliferative and heterogeneous tumors which have proven quite difficult to treat. This work will first examine the potential for the transmembrane glycoprotein CD133 to be a hallmark of human glioblastoma CSCs. CD133, also referred to as Prominin-1, is a 5-transmembrane glycoprotein of 117 kDa encoded by a gene on chromosome 4p15. It is expressed by hematopoietic progenitor cells, embryonic stem cells, and various cancers[7].

While it is thought to be responsible for orchestrating cell-cell topography, neither its ligands nor its actual function are certain[8]. However, cells expressing CD133 have been shown to have self-renewing and differentiating ability *in vivo*; it has been used to identify putative cancer stem cell populations from malignant brain tumors, as well as other types of cancers[9].

However, $CD133^-$ CSCs have also been isolated and shown to form tumors[10]. It is possible that these cells harbored an occult population of expressed CD133 protein that wasn't realized, perhaps because of differential folding resulting from differential glycosylation masking specific CD133 epitopes[11]. This makes detection of expressed CD133 using antibodies difficult; it suggests the possibility that what is described as a $CD133^-$ population is actually a population of cells that is $CD133^+$ but with differing glycosylation status[12]. In addition, difficulty in identifying the CD133 molecule could

also be due to local tumor microenvironment[13], or epigenetic modifications, such as promoter methylation[14]. What is also problematic is that the majority of $CD133^+$ cells are characterized by having significantly higher levels of expression of O6-methylguanine-DNA-methyltransferase, or MGMT, compared to $CD133^-$ cells [15]. MGMT is a DNA repair protein and is the chief antagonist to Temozolomide (TMZ), the most frequently employed antitumor alkylating agent. Methylation of the MGMT promoter has been shown to both increase chemosensitivity to alkylating agents[16,17] and to correlate with an improved response to radiotherapy[18]. Thus, cells with higher levels of CD133 correlate with antitumor drug resistence[19], and resistance to radiotherapy[15].

Therefore, the evidence points to $CD133^+$ cells being a hallmark of GBM CSCs.

CD147

While the role of CD133 is unclear, the CD147 molecule (basigin) has been well described. CD147 is a 385-amino acid molecule with a molecular weight of 42 kDa found on the surface of many types of cells, including leukocytes, epithelial and endothelial cells. It is an integral membrane protein belonging to the immunoglobulin superfamily of proteins, and as such plays an essential role in intercellular recognition[20]. CD147 is also highly glycosylated giving the protein an apparent MW of around 60 kDa. Additionally, CD147 regulates the expression of the monocarboxylate transporter (MCT) family of proteins. MCTs are responsible for shuttling lactic acid out of highly malignant tumors which rely on anaerobic glycolysis as an energy source[21]; without MCTs the

resulting buildup of lactate would acidify the cell cytoplasm and slow or stop cellular metabolism.

One of the best-described functions of CD147 is its ability to induce expression of matrix metalloproteinases (MMP) in stromal cells[22]. It is from this function that its alternate name, EMMPRIN (Extracellular Matrix MetalloPRoteinase Inducer), is derived. Matrix metalloproteinases are from a large family of proteins and have many differing functions, but we are chiefly concerned with their pathophysiologic functions, such as modulation of tumor microenvironment. In this capacity MMPs are essential for cell growth, angiogenesis, inflammation, and tumor cell migration[23]. Thus, CD147 induces expression of molecules which support tumor growth and increase lethality and aggressiveness of tumors. Under the relatively-hypoxic conditions, the conditions employed in this study, CD147 promotes tumor growth, enhances tumor malignancy, and inhibits tumor cell apoptotic ability[24].

CD147 up-regulates MMP secretion by adjacent stromal cells, which in turn degrade the extracellular matrix. Thus, CD147 is a key element in tumor invasion, metastasis, and progression.[25]. It has been shown that CD147 is overexpressed on the surface of GBMs, and further, that relative level of CD147 expression is correlated with WHO grade of astrocytoma[26]. These findings suggest that CD147 is a worthwhile therapeutic target.

Hypoxia

Currently, GBM tumors are treated by surgical removal and subsequent treatment with both chemotherapy and radiotherapy. One agent mitigating the effects of these latter two treatments is intratumoral hypoxia[27]. TMZ, the most-used anti-GBM drug, has been found to target only GBM cells derived from the peripheral layer of the tumor mass[28]. The interior-most cells, the cells exposed to the least amount of circulating oxygen, have proven the most resistant to the alkylating agent treatment. These data suggest that there is a direct correlation between intratumoral hypoxic gradient and resistance of the tumor cells to chemotherapeutic agents.

In normal brain tissue, physiological concentrations of oxygen will vary between 0.5 and 7.5%. In GBM tissue, however, this value is markedly decreased to as little as 0.1% or less[29], suggesting hypoxia is an agent of GBM. The hypoxic microenvironment plays a key role in the regulation of the CSC phenotype; exposure of GBM cells to hypoxic conditions encouraged a phenotypic shift of cells toward a more stem-like state, and these alterations were in turn accompanied by upregulation of markers of undifferentiated cells, such as Oct4, and neural stem cell markers, like nestin[30]. Additionally, hypoxic culturing also induces a phenotypic shift to one of increased glycolytic activity; the cells undergo a metabolic reprogramming which ultimately results in acidification of the tumor microenvironment. This acidic environment induces upregulation of stem-cell genes such as VEGF[31], and Olig2, Oct4, and Nanog[32]. Thus, hypoxia induces phenotypic shifts towards stemness.

Objectives

The literature suggests that the respective relative overexpression of CD133 and CD147 antigen causes increased tumorigenicity. We examined this potential property through direct comparison of high- and low-expressing cells of each antigen. The aim of this work was to isolate a subpopulation of $CD133^{+}$ human GBM cells and measure their ability to form neurospheres in stem cell-culture suspension. In parallel, populations of cells expressing various levels of CD147 were isolated to measure similar properties.

EXPERIMENTAL DESIGN

Subculture of Human GBM Cell lines

LN229, T98, and U87MG adherent cell lines (American Tissue Culture Collection, Manassas, VA) were removed from cryostasis in liquid nitrogen and resuscitated. Per standard culturing methods, the T98 and U87MG lines were cultured in Eagle's Modified Essential Medium (EMEM; Lonza, Walkersville, MD) with 10% Fetal Bovine Serum (FBS; Atlanta Biological, Atlanta GA); the LN 229 in Dulbecco's Modified Eagle's Medium (DMEM; GE Life Sciences, Logan, UT) with added 5% FBS (Atlanta Biological). Both media were supplemented with 1% Penicillin-Streptomycin-Amphotericin B (PSA; Gibco, Carlsbad, CA) antibiotics. Cells were kept in cryostorage in 1ml aliquots in freeze medium (90% FBS, 10% DMSO); each aliquot was added to 19ml of appropriate, pre-warmed complete culture medium in $75cm^2$ tissue-treated culture flasks under laminar flow. Each was placed in incubation at 37^0 C and 5% CO_2 until near-confluency (~75%) was reached, at which point the respective flasks were either passaged (subcultured) or cells were harvested for use. After one passage for each cell line, cells were then transferred to $175cm^2$ flasks to increase total number of cells available for RNA extraction and cell sorting. Cells were then kept in $175cm^2$ flasks throughout the duration of the experiments.

To create a microenvironment which would potentially cause a phenotypic shift towards a more stem cell-like state, after several passages, the cells were transferred from

normoxic conditions to the hypoxic (5% CO_2, 5% O_2) incubator en masse and remained there throughout the remainder of the study.

Extraction of mRNA

Once near-confluency had been achieved, cells were removed from respective flasks with trypsin-versene (Lonza) and pelleted at 300 rcf for 10 minutes. RNA was extracted from each cell line independently using an RNA/DNA/Protein AllPrep kit (Qiagen, Valencia, CA) following manufacturer's protocol. Pelleted cells had supernatants removed and pellets were resuspended in 350µl Buffer RLT, and vortexed several seconds to mix. Lysates were then homogenized using centrifugation at 14000 rpm (top speed) for 2 minutes using a tabletop centrifuge in conjunction with QiaShredder (Qiagen, Valencia, CA) spin columns. After, lysates were transferred to Allprep DNA spin column placed in 2ml collection tube and centrifuged at top speed 30 seconds. The flow through from each sample was then combined with 250µl 100% ethanol and mixed by pipetting. Samples were then added to separate RNeasy spin columns in a 2ml centrifuge tube and centrifuged at top speed 15 seconds. To each column 700µl Buffer RW1 was added, and each tube centrifuged at top speed for 15 seconds. After, 500µl Buffer RPE was added to each column and centrifuged at top speed for 15 seconds. This step was then repeated but centrifuged for 2 minutes to ensure complete drying of the column. Columns were then removed and replaced in 1.5ml

collection tubes. To each, 10µl of RNase-free H_2O was added, and the columns were then centrifuged at top speed for 1 minute.

If reverse transcription was not performed immediately after extraction, RNA was stored at -20°C. Storage at -20°C was limited to one week or less.

Reverse Transcription

To convert the extracted RNA into cDNA, reverse transcription was performed using avian myeloblastosis virus reverse transcriptase (AMV-RT) and the manufacturer's protocol (Promega, Madison, WI). Exactly 2µg of RNA was combined with 2µl of either oligo dT primers (Promega, Madison, WI) or random hexamer primers (Promega, Madison, WI). The amount in microliters varied and depended upon concentration of RNA extracted from respective cell lysates; volumes did not exceed 8µl as total volume of primer/RNA cannot exceed 11µl and the ratio of primer to template RNA cannot be altered. Solutions containing oligo dT primers were incubated at 42°C and those containing random hexamer primers were incubated at 37°C at a ratio of 0.5µg primer/µg RNA in a sterile, nuclease-free 200µl microcentrifuge tube. This mixture was placed in a Thermal Cycler (BioRad T100, BioRad, Hercules, CA) and heated to 70°C for 5 minutes, then chilled to 4°C for 5 minutes. After, the primer/template mixture was kept on ice, and the following were added in order:

5µl AMV RT 5X Reaction Buffer
2.5µl dNTP Mix
30 units AMV RT (at 10 units/µl; 3µl AMV RT added)

dH_2O sufficient to bring total volume to 25µl (amount varies depending upon volume of RNA added)

The samples were then incubated for 60 minutes at the appropriate temperature described earlier. The cDNA products were stored at -20°C for later use, if not used immediately.

PCR

The cDNA obtained via reverse transcription was used to amplify the CD133 gene using endpoint PCR. Thermal Cycling parameters were in accordance with the PCR Master Mix protocol (Promega, Madison, WI). Reactions of 25µl were set up as follows:

12.5µl PCR Master Mix (Promega)
10.0µl Nuclease-free H_2O
1.25µl of each primer (forward and reverse)
2.25µl cDNA template

Parameters for the PCR amplification were as follows:

2 minutes at 95°C
1 minute at 51°C (5°C less than lowest T_m of primers)
1 minute at 72°C (optimal temperature for Taq polymerase)

This cycle was repeated a total of 35 times, after which a final extension of 5 minutes at 72°C was performed. After, samples were cooled to 4°C and examined immediately or placed at -20°C until analyzed. Storage at -20°C was limited to one week or less.

PCR Primer Design

Primer sets used were designed using Primer3 on My Biology Workbench (http://workbench.sdsc.edu/). PrimerBlast was employed subsequently to ensure specificity to target genes, and finally the IDT OligoAnalyzer tool (www.idtna.com) was used to ensure favorable annealing to target sets and to preclude formation of primer-dimers.

Table 1. IDT primer sets used for endpoint PCR and qPCR

Primer (Human)	Sequence (5′-3′)
CD133(1) forward	GTC CTG GGG CTG CTG TTT AT
CD133(1) reverse	TCC TTG ATC GCT GTT GCC AT
CD133(2) forward	CCT GGT CCA ACA GGG CTA TC
CD133(2) reverse	GAA GGA CTC GTT GCT GGT GA
CD133(3) forward	GCC AGC CTC AGA CAG AAA AC
CD133(3) reverse	CCA AGC CTT AGG AGC ATC TG
Basigin-2 forward	GCG GTT GGA GGT TGT AGG AC
Basigin-2 reverse	GGG AGG AAG ACG CAG GAG TA
GAPDH forward	AAG GTC GGA GTC AAC GGA TTT GGT
GAPDH reverse	AGT GAT GGC ATG GAC TGT GGT CAT

Gel Electrophoresis

A 1% agarose gel electrophoresis was subsequently used to detect for the presence of DNA products synthesized during endpoint PCR. The gel was created by combining 0.25g agarose and 25ml TBE (Tris/Borate/EDTA) buffer and heated until

agarose dissolved. After cool enough to touch, 1µl 10µg/µl ethidium bromide was added and mixed. Mixture was poured into standard gel box setup. PCR products were added and run at 120V for 45 minutes in 1X TBE buffer. Gel bands were visualized using Gel Doc Imaging System (BioRad, Hercules, CA).

Fluorescence Activated Cell Sorting (FACS)

Culture cells were evaluated for CD133 or CD147 expression using the S3 Cell Sorter (BioRad, Hercules, CA).

For the CD133 FACS, the culture cells (LN 229, T98, and U87MG) were first removed from the respective culture flasks with 8ml trypsin-versene (Lonza) or Accutase (Innovative Cell Technologies, San Diego, CA) and resuspended in 16ml complete medium. The respective cell suspensions were then centrifuged at 800 rcf for 5 minutes. Supernatants were aspirated and pellets were resuspended in 2ml sort buffer [1X Ca/Mg free PBS (Fisher Scientific, Pittsburgh, PA), 1% BSA (HyClone, Logan, UT), 25mM HEPES (HyClone, Logan, UT), pH 7.0] and centrifuged as before. Supernatant was aspirated and pellet resuspended in 120µl sort buffer. A 20µl sample of the cell suspension was removed for use as a control sample. To the remaining 100µl of cell suspension, 10µl of CD133 antibody (AC133-Viobright FITC, Miltenyi Biotec, San Diego CA) was added in dark conditions. The mixture was allowed to incubate in darkness at 4^{o}C for 10 minutes, according to the manufacturer's suggestion. Following incubation, sample was centrifuged at 300 rcf for 5 minutes, supernatant removed, and

pellet resuspended in 1ml sort buffer. This volume was increased to 4ml with sort buffer, and control sample volume increased to 1ml with the same. Both samples were separately strained twice using a 40µm cell strainer.

For the CD147 FACS, U87MG cells were removed from flasks using trypsin-versene, resuspended in the same medium as above. The cells were then centrifuged at 850 rcf for 6 minutes. The supernatant was aspirated and pellets resuspended in 1.5ml sort buffer and centrifuged as before. Supernatant was removed and pellets resuspended in 100µl sort buffer. A 10µl sample was removed for use as a control sample. To the remaining 90µl, 20µl of anti-CD147 reagent was added (MEM-M6/1) FITC Mouse mAb; Novus Biologicals, Littleton, CO). The sample was then incubated at 4°C for 60 minutes in darkness. Following incubation, samples were centrifuged at 400 rcf for 5 minutes. Supernatants were removed and pellets resuspended in 1.2ml sort buffer, then recentrifuged as before. This step was performed twice. Supernatants were then aspirated, and pellets resuspended in 1ml sort buffer. Working samples and control samples were brought to 4ml and 1ml volumes respectively with sort buffer and strained twice as above.

In either case, before FACS the control samples were run through the sorter to acquire fluorescence data for the untreated cells as a basis for comparison with the fluorescent antibody-labeled cells. Once a standard had been established, new data were acquired on the treated cells and a new standard established; unlabeled and antibody-labeled cells were then sorted and collected based on this standard, using the ProSort v1.2 Software (BioRad, Hercules, CA).

Cells sorted for CD133 expression were sorted based on fluorescence to any degree. This value is measured by the FACS instrument via photon emission. Unlabeled cells simply pass by the laser in the instrument and emit no photons, thus no signal will be detected. As fluorescent antibody-labeled cells pass by the laser, photons are emitted and the intensity of the voltage measured by the instrument increases. These data are displayed in the form of histograms, which plot a single parameter (i.e. FITC intensity, x-axis) against event number (y-axis); and scatter-plots, which plot two parameters simultaneously: side-scatter intensity (y-axis) against fluorescence intensity (x-axis), with each dot representing a single event. The x-axis shows relative fluorescence on a logarithmic scale, with each successive "decade" representing a relative tenfold increase in measured fluorescence. After antibody labelling, data were acquired on 100,000 events. On the resulting histograms, sorting gates were placed to collect the lowest-20% fluorescing and highest-20% fluorescing cells in each sample; this percentage is indicated numerically in the "statistics" window of the histogram plots.

Using these parameters, CD147 expression was divided into two groups: lowest-20% expression ("low expression") and highest-20% expression ("high expression").

Subculture of Sorted Fractions

The U87 cells labeled with anti-CD147 antibody were sorted into "high" and "low" fractions; the "low" fraction consisted of the 20% lowest-fluorescing (and therefore, lowest-CD147-expressing) cells in the sample. The "high" fraction consisted of

the 20% highest-fluorescing. From either fraction, 300,000 cells were placed in adherent culture (FBS-supplemented medium) and same number of each placed in suspension culture using complete stem cell medium [DMEM/F-12 with L-glutamine (Gibco, Carlsbad, CA), 2% StemPro Neural Supplement (SPNS; Gibco), 20% Epidermal Growth Factor (EGF; Preprotech, Rocky Hill, NJ), 20% Basic Fibroblast Growth Factor (bFGF; Preprotech, Rocky Hill, NJ), 10mg/ml Gentimicin (Gibco), 0.5% PSA (Gibco), 0.5mg/ml BSA (HyClone, Logan, UT)]. In both cases, 25cm^2 flasks were used, each containing 4ml of appropriate medium. After 96 hours of incubation in hypoxic conditions at 37°C, cultures were observed for relative level of proliferation, neurosphere formation (suspension culture) or total cell count (adherent culture).

For counting the adherent cells, cells were treated with 2 ml trypsin-versene solution and allowed to incubate in hypoxia for 3 minutes, after which each flask was placed back into the laminar flow hood and gently scraped for 30 seconds to remove any remaining adhered cells. To this cell/trypsin solution, 6ml of EMEM complete medium was added. After mixing by pipetting, the respective cell solutions were removed and placed into 15ml conical tubes for cell counting. To a 100µl sample of each, Trypan Blue dye was added at 1:6 dilution and cells were counted using a hemocytometer and standard protocol.

Additionally, a subsequent sort was performed collecting the highest- and lowest-1% CD147-expressing cells. These fractions were used exclusively for qualitative examination using a confocal microscope.

Real-Time PCR Analysis of Sorted Fractions

U87MG cells were sorted into high- and low-fluorescing fractions as described. Respective fractions were combined in conical tubes and centrifuged at 300 rcf for 10 minutes. Supernatants were aspirated, and RNA was extracted, reverse transcription performed as described above. The cDNA obtained was amplified employing qPCR using a LightCycler 2.0 (Roche Diagnostics, Indianapolis, IN). For this analysis, CD133, CD147, and GAPDH genes were examined, the last being used as a control. This instrument employs colorless glass capillary tubes and a carousel; each tube houses 20µl of sample.

To the negative controls, 16µl PCR-grade H_2O was added, followed by 2µl of primers and 2µl LightCycler DNA Master SYBR Green I reagent (Roche Diagnostics, Indianapolis, IN). After, 14µl of PCR-grade H_2O was added, followed by 2µl of primers and 2µl of SYBR Green I reagent, to separate thin-walled PCR tubes kept on ice. The samples were mixed by pipetting, and then transferred to the capillary tubes contained within centrifuge adapters, themselves contained within a cold block. All samples were then centrifuged 30 seconds at 500g before being added to the LightCycler. The qPCR was run using the following parameters:

Denaturation: 1 Cycle, 95°C, 30 seconds
Amplification: 45 Cycles: Denaturation: 95°C, 0 seconds
Annealing: 51°C, 5 seconds
Extension: 72°C, 30 seconds
Cooling: 1 Cycle, 40°C, 30 seconds

The data were analyzed using proprietary LightCycler software v. 4.05 (Roche Diagnostics, Indianapolis, IN).

Immunocytochemistry Analysis of CD133 Antibody using HF2303 Cancer Stem Cells

Qualitative analysis of the anti-CD133 antibody (Miltenyi, San Diego, CA) was performed using a confocal microscope (Olympus Fluoview FV1000 Confocal Laser Scanning Microscope, FV10-ASW 3.1 software; Olympus Corporation Americas, Center Valley, PA). HF2303 primary human GBM cancer stem cells (Henry Ford Hospital, Detroit, MI) were cultured at 37°C in hypoxia using complete stem cell medium [DMEM/F-12 with L-glutamine (Gibco, Carlsbad, CA), 2% StemPro Neural Supplement (SPNS; Gibco), 20% Epidermal Growth Factor (EGF; Preprotech, Rocky Hill, NJ), 20% Basic Fibroblast Growth Factor (bFGF; Preprotech, Rocky Hill, NJ), 10mg/ml Gentimicin (Gibco), 0.5% PSA (Gibco), 0.5mg/ml BSA (HyClone, Logan, UT)]. 10ml of medium (with suspended cells) was removed and placed in a 15ml conical tube. This was centrifuged at 150rcf for 90 seconds. Then 9.4ml of the supernatant was aspirated, leaving 0.6ml supernatant and HF2303 cells. The cells were resuspended and divided, and 300µl was added to each well of one gasketed coverslip (CultureWell MultiWell Chambered Coverslips, Grace Bio Labs, Bend, OR).

Coverslip wells were pretreated by adding 100µl Poly-d-Lysine (BD Biosciences, San Jose, CA) to each well. After 10 minutes, the Poly-d-Lysine was removed and then the cell suspension was added. The cells were allowed to incubate on the coverslip 6 hours at 37°C in hypoxia. After, the wells were removed of medium and washed twice with 1X PBS. Then 400µl blocking buffer (5% BSA, 0.1% Triton X-100 in PBS) was added and allowed to incubate under laminar flow for 20 minutes at RT. In a darkroom under red safe light, 400µl of anti-CD133 antibody was added (1:1000) and allowed to

incubate in darkness at room temperature for 60 minutes. The antibody solution was then removed and wells were washed twice with wash buffer. This was removed and 400µl 4% paraformaldehyde solution was added and allowed to incubate for 20 minutes at RT. Wells were then washed twice with 1X PBS. PBS was then removed, silicon gaskets removed, and coverslips gently waved to air-dry. One drop per well of ProLong Diamond Antifade Mountant with DAPI (ThermoFisher Scientific, Waltham, MA) and coverslips were then mounted to slides. Slides were wrapped in foil and allowed to stand at RT overnight (>12 hours).

Immunocytochemistry Analysis of High and Low CD147-expressing U87MG Cells

Further qualitative analyses of the sorted U87MG cells was performed using a confocal microscope (Olympus Fluoview FV1000 Confocal Laser Scanning Microscope, FV10-ASW 3.1 software; Olympus Corporation Americas, Center Valley, PA). The slides were manufactured using gasketed coverslips as before (CultureWell MultiWell Chambered Coverslips, Grace Bio Labs, Bend, OR). Two slides were made using U87MG cells sorted based on relative expression of CD147. The first contained the highest- and lowest-20% of CD147-expressing cells, and the second slide contained the highest- and lowest-1% of CD147-expressing cells.

Of each cell type, 10,000 were added to a different coverslip well, which were pretreated with Poly-D-Lysine (BD Biosciences, San Jose, CA) as described above. The gasketed coverslips were allowed to incubate 6 hours at 37°C in hypoxia. After, 400µl of

4% paraformaldehyde in PBS were added and allowed to incubate for 20 minutes at RT. Wells were then washed twice with 1X PBS. PBS was then removed, silicon gaskets removed, and coverslips gently waved to air-dry. One drop per well of ProLong Diamond Antifade Mountant with DAPI (ThermoFisher Scientific, Waltham, MA) and coverslips were then mounted to slides. Slides were wrapped in foil and allowed to stand at RT overnight (>12 hours).

Statistical Analysis

Data obtained from adherent U87MG proliferation assay were expressed as mean and standard error. Data were analyzed by paired two-tailed t-test; calculations were performed using Microsoft Excel. Data were considered significant at $P < 0.05$.

RESULTS

Identifying presence of CD133 transcripts in LN229, T98, and U87 cell lines

After RNA extraction, reverse transcription and subsequent endpoint PCR, agarose gel electrophoresis was performed using the three CD133 primer sets to determine the presence of CD133 DNA in the LN229, T98, and U87 cell lines. The results indicate that the CD133 transcript is present in the cell lines and therefore could be employed as a potential marker for cancer stem cells.

The data in figure 1 show bands present in lanes 4, 7, and 10 between 200-300bp relative to the ladder; the product size for primer set 3 is 247bp which suggests the presence of CD133 DNA across all three cell lines. Primer set 3 was used exclusively henceforth due to its smaller size and ubiquity. A redundant agarose gel analysis was subsequently performed (Figure 2), which confirms the success of this primer set.

Confocal Imaging of CD133 Protein Expression in Cancer Stem Cells

Because the literature indicates that levels of CD133 may be low among the general population of GBM cells[2,5,8,10-12], the antibody (CD133/1 (AC133) Viobright FITC; Miltenyi Biotech, San Diego, CA) used to detect CD133 was tested on HF2303 cells which ubiquitously express the CD133 antigen[33]. The image shows almost complete

binding of the antibody to the HF2303 cells, therefore suggesting the antibody indeed binds to CD133 antigen (Fig. 3).

Identification of GBM Cells Positive for CD133

Using the methods described, the LN 229, T98 and U87MG cells were pre-labeled with the FITC-conjugated anti-CD133 antibody and then sorted based on relative fluorescence compared to unlabeled cells. Each sort yielded extremely low numbers of cells which had shifted downstream far enough to be considered fluorescing; often these numbers were two-figure or even single digit values. Commonly, ~0.03% of cells were labelled by the antibody. Multiple sorts performed across all three cell lines yielded similar results.

There is very little difference in either the histogram plots (Fig. 4-5) or the side-scatter plots (Fig. 6-7). Only several cells are displayed (Fig. 7) beyond the second decade, where fluorescing cells would likely be, based on the fluorescence data acquired before the antibody was introduced. These data indicate that while the cells were expressing CD133 mRNA, CD133 could not be detected on the surface of the cell using this method.

Sorting of U87MG Cells Based on Expression Levels of CD147

To ensure presence of CD147 on the target cells and successful binding of antibody/fluorescence of FITC conjugate, U87MG cells were cultured overnight with antibody and photographed using a fluorescent microscope. The data suggest the presence of CD147 on the cell surface and that successful sorts may be performed using these methods (Fig. 8).

U87MG cells were pre-labeled with anti-CD147 antibody with FITC conjugate and sorted into high and low fractions. The initial sort yielded an identically-split population; half the cells were expressing, half were not. Subsequent sorts found that most cells were fluorescing relative to the unlabeled cells; about 99% on average. While the cells displayed little or no expression of CD133, they exhibited nearly universal expression of CD147.

After the cells were incubated with the anti-CD147 antibody, a clear shift is noticeable in the histogram plot (Fig. 9-10). In the initial plot, the fluorescence peak (representing presence of cells) is contained almost entirely within the first decade of the area log. After antibody addition, roughly 90% of the fluorescence peak is located beyond the first decade, indicating a significant increase in the level of fluorescence relative to the unlabeled U87MG cells. Therefore, a vast majority of the cells expressed the CD147 antigen.

In similar fashion, the scatterplots of the pre- and post-antibody-labeled U87MG cells display a clear downstream shift in the cell concentration (Fig. 11-12). Blue areas indicate the areas of highest cell concentration. After the U87MG cells were labelled with

the anti-CD147 antibody, the cell population had clearly exhibited a tenfold increase in level of fluorescence relative to the unlabeled U87MG cells. Thus, a majority of the U87MG cells tested were bound by antibody, indicating presence of CD147 on a vast majority of the cells.

Cells with Increased CD147 Expression Form Neurospheres in Suspension Culture

After sorting into fractions, collected high- and low-CD147-expressing U87MG cells were collected and placed into suspension culture using complete stem cell medium. The cells were placed in hypoxia at 37°C and allowed to remain for four days. After 96 hours incubation time, the culture flasks were photographed using a light microscope. This was repeated two additional times, for a total of three groups of (high and low) expression culture (Fig. 13-18). The cells expressing the higher levels of CD147 had formed large neurospheres after incubating 96 hours in hypoxia. In the cultures of cells expressing relatively low CD147 levels, no neurospheres had formed. The suspension cultures of low-expressing CD147 remained as singlet cells; there were only rare instances of even doublets formed by these cells.

Adherent Cultures of High-CD147 Cells are More Proliferative

Fractions of U87MG cells expressing both high and low levels of CD147 (20% highest-expressing/20% lowest-expressing) were also separately added to adherent cell

culture and allowed to proliferate. After 96 hours, cells were counted using standard manual methods. To preclude bias, identity of respective flasks was hidden and revealed to the author after results were tallied. In all three sets of cultures, the U87MG cells expressing relatively higher levels of CD147 were more proliferative (Figure 19). The mean values for each group were calculated. The mean concentration of cells in the high-expressing group was 4.245 million cells/ml; in the low-expressing group this value was 1.665 million cells/ml. Thus, the high-expressing group showed a 245% increased growth rate compared to the low-expressing group of U87MG cells.

qPCR Data Suggest Increased CD147 Levels and Increased CD133 Levels are Correlated

CD133 and CD147 gene expression was assessed by qPCR. ΔCT levels were recorded for CD133 and CD147 relative to GAPDH. The ΔCTs for the CD147 levels in the high and low fractions were 8.38 and 6.67, respectively, for a positive ΔΔCT of 1.71. While it is interesting that the low-CD sample had a slightly lower CT, these values indicate strongly positive reactions with abundant CD147 gene expression. The values also indicate relatively high levels of CD147 in general, relative to the CT of GAPDH. The respective ΔCTs in the high-CD147 (ΔCT=16.86) and the low-CD147 (ΔCT=19.79) samples of CD133 were also strongly positive, suggesting relatively high levels of CD133 gene expression in both samples. The ΔΔCT for these samples is 2.93, with an expression fold change of 7.62. Thus, CD133 was expressed 7.62 times more in the high-CD147 sample compared to the low-CD147 sample. These data indicate that CD133

gene expression is present in U87MG cells, and that high-CD147 levels may strongly correlate with elevated expression of CD133.

Laser Confocal Imaging of Sort Fractions Confirms Expected CD147 Levels Based On Sort Parameters

Cells from either high or low sort fractions were added to gasketed coverslips, fixed with 4% paraformaldehyde, and mounted to slides using DAPI-containing mounting medium. The U87MG cells expressing highest levels of CD147 all exhibit green coloration (FITC, attached to anti-CD147 antibody) at areas close to but distinctly separate from the cell nuclei (Blue, DAPI-stained) (Fig. 20). Because the highest-20% fraction fluoresce at high levels per the sort data, the cells collected in the higher expressing fraction of U87MG cells should all be labelled with FITC; the confocal images suggest the same.

Conversely, we expect that the low CD147-expressing fraction of U87MG cells collected would have some FITC expression visible under microscopy, though not all. Based on fluorescence data from sorting, the low population does include U87MG cells that either do not express surface CD147 or express at low enough levels that the fluorescence was not detected. Lastly, the low population would include cells which simply did not bind antibody for any reason. Some low CD147-expressing cells certainly express CD147, based on FITC fluorescence. Other U87MG appeared to express little CD147. Yet other labelled U87MG cells appeared to be expressing no CD147 whatever, or at least did not appear to fluoresce (Fig. 21).

To streamline this approach relative to this experiment, microscope slides were prepared with the highest- and lowest-1% fractions from FACS and U87MG cells labeled with the same anti-CD147 antibody as described. The highest 1% population exhibits universal basigin expression as indicated by the green fluorescence (FITC) (Fig. 22). None of the cells in the lowest-1% fraction are exhibiting any detectable levels of fluorescence, suggesting that isolating these two extreme populations for study is possible (Fig. 23).

DISCUSSION

While it has been shown that stem-like cancer cells may be cultured successfully using adherent or suspension conditions[35,37], and that U87MG cells form neurospheres in suspension culture[36-37], a correlation between U87MG/GBM neurosphere formation and CD147 levels may be a novel finding. We have shown here that U87MG GBM cells expressing relatively high levels of CD147 on the cell surface are both more proliferative and more likely to form neurospheres than their lower-expressing counterparts. All three suspension cultures of U87MG cells expressing high levels of CD147 formed large neurospheres in culture after only four days, and none of the cells expressing low levels of CD147 formed neurospheres after the same time period. These data suggest that CD147 levels are directly correlated with neurosphere formation in GBM cells, or that the CD147 levels are indicative of some other such agent of neurosphere formation.

We attempted to show that CD147 is a cancer stem cell marker in order to establish it as a worthwhile target for antitumor therapy. The evidence presented here has validated our attempts. Because CD147 is not typically found on glial cells and neurons, it can be employed to delineate normal, healthy tissue from cancerous tissue. Chemotherapeutic agents targeting CD147 would not only be a highly effective form of treatment, but targeting this population of cells would not affect healthy tissue surrounding the tumor mass, bypassing a major hurdle confronted during surgical excision.

Preliminary data recorded performing qPCR on the high and low sort fractions suggests that CD133 overexpression on U87MG cells is correlated with CD147 overexpression. While this was preliminary data performed from cDNA collected from a single sort and must be confirmed and reconfirmed, CD147 overexpression may positively affect $CD133^+$ CSC enrichment. It is possible that the cells are geared toward expressing relatively high levels of the CD133 antigen but epigenetic factors and posttranslational modifications prevent this expression from being realized[14]. Because inhibition of the Sonic Hedgehog pathway in $CD133^+$ cells enhances the effectiveness of the chemotherapeutic agent temozolomide[37], identifying this population of cells based on CD147 expression would be quite effective.

RNA extraction and subsequent reverse transcription and endpoint PCR indicate that the transcripts for CD133 are present among all three GBM cell lines used throughout these experiments. Therefore it was expected that sorting LN229, T98, and U87MG cells based on relative levels of CD133 antigen expression should be possible. It is not clear that the GBM cell lines do not express the CD133 antigen. It is possible that the trypsin-versene and Accutase used to remove the cells from the culture flask may cleave the AC133 epitope, which may require a longer period of time devoted to cell recovery before the addition of antibody. While the manufacturer of the antibody (Miltenyi) insists that 10 minutes is sufficient time for antibody binding, it may be prudent to increase the incubation time, which may improve binding. This approach will also help address any issues regarding recovery period of the epitope following trypsinization/collagenization with Accutase. Non-enzymatic removal of the cells from the flask seemed like a logical alternative to treatment with proteinase or collagenase and

may leave the CD133 antigen intact. However this removal method was not deemed viable as it was impossible to separate the cells, which is necessary for sorting.

Furthermore, as stated earlier it has been suggested[11] that the CD133 antigen may be expressed on the cell surface, but precluded from binding to the antibody due to steric hindrance or similar problems. However, the correlation suggested by these data indicates that by selecting for a population of U87MG cells expressing increased levels of CD147 we also enrich a population of $CD133^+$ cells. Thus, it would certainly be possible to sort a high-CD147 population of U87MG cells and in turn label those cells with the anti-CD133 antibody. This approach should significantly increase the percentage of $CD133^+$ cells while also precluding any problems like steric hindrance of antibody binding, cleavage of AC133 epitope, etc.

Future Directions

To confirm if CD147 expression is responsible for neurosphere formation and adherent-cell proliferation as the data suggested here, it would be prudent to employ the CRISPR Interference technique to repress CD147 expression. The Clustered regularly interspaced short palindromic repeats (CRISPR) pathway is a genetic perturbation technique which affords transcriptional-level sequence-specific activation or repression of gene expression, similar to RNA Interference[38]. This technique can repress transcription by blocking transcriptional initiation or elongation, or inducing heterochromatization; it has been shown to generate gene knockouts in humans[39]. Thus,

this technique could be used to knock out CD147 expression in U87MG cells. Then, drawing on the correlation established here, these cells could be sorted based on relative levels of CD133 expression; the $CD133^{+}$ group would otherwise be identical to the high-CD147 U87MG cells used here, save CD147 expression. These cells would then be suspension-cultured as performed here and observed for neurosphere formation.

Secondly, to confirm or disconfirm the effects of hypoxia on CD147 expression/ neurosphere formation, the experiment should be repeated with U87MG cells incubated only in normoxia. If neurospheres reform it might suggest that either the relative expression levels of CD147 are not driven by environmental oxygen levels, or that the levels of CD147 expressed in normoxia are sufficient to drive neurosphere formation, assuming CD147 is indeed the agent of neurosphere formation herein. Repeating the experiment in normoxia followed by CRISPR knockout of CD147 expression would further illustrate the role CD147 plays in proliferation and formation of neurospheres in U87MG cells. Additionally, once the experiment has been repeated and neurosphere formation observed, the neurosphere assay should be performed to confirm the ability of the cells in the neurosphere to proliferate and self-renew, and to assess their potency level.

In conclusion, we have demonstrated here that U87MG cells can be sorted based on relative levels of CD147 expression. We have shown that U87MG cells expressing relatively high levels of CD147 will form neurospheres when incubated in suspension culture in hypoxia. We have also shown that U87MG cells expressing high CD147 levels are more proliferative in adherent culture than low-CD147 expressing U87MG cells. We have also supplied preliminary data which may suggest CD147 overexpression and

CD133 overexpression in U87MG cells are correlated, and it is possible that these two conditions in conjunction cause increased proliferation and neurosphere formation. Thus, CD147 and CD133 are worthwhile targets for GBM therapy going forward.

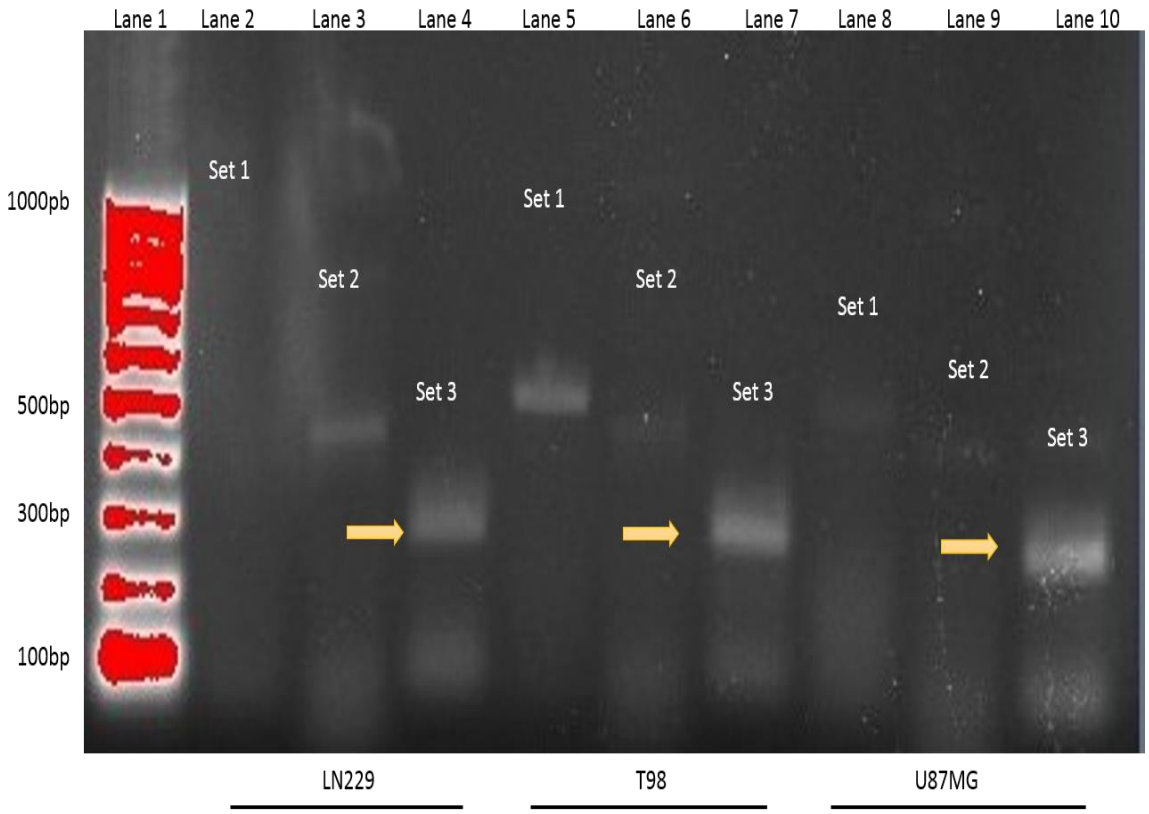

Figure 1. Agarose gel electrophoresis analysis of LN229, T98, and U87MG PCR products using CD133 primers. Arrows indicate bands from Set 3 between 200-300bp.

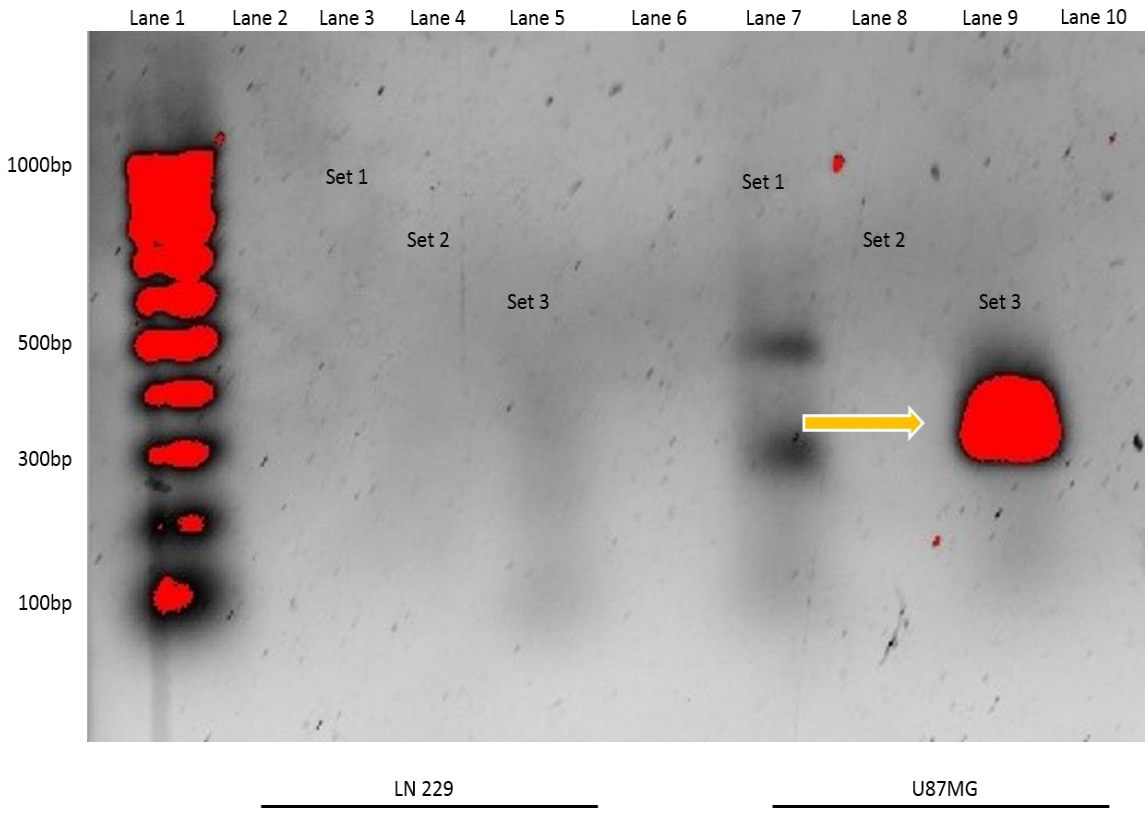

Figure 2. Comparison of LN229 and U87MG cells displaying bands after PCR performed with the three CD133 primer sets. Primer set 3, in lane 9, displays dark band in 200-300bp range (arrow).

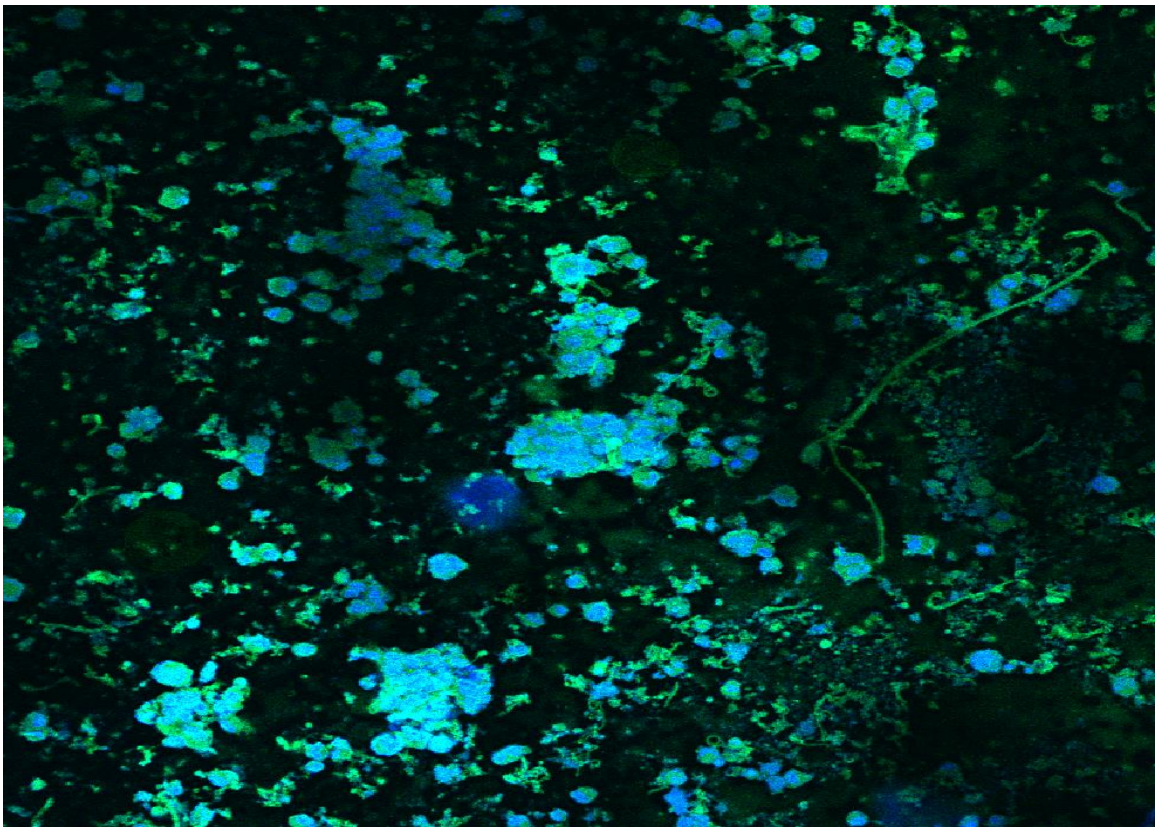

Figure 3. HF2303 neurospheres express the stem cell marker CD133. Neurospheres stained with DAPI (blue) and examined under confocal laser microscopy. Cells labelled with anti-CD133 antibody with FITC conjugate (green).

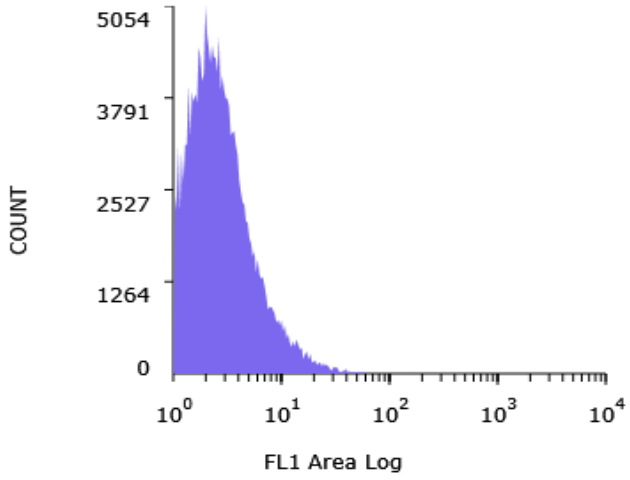

Figure 4. Fluorescence data of T98 cells before labelling with anti-CD133 antibody. Data acquired using S3 sorter.

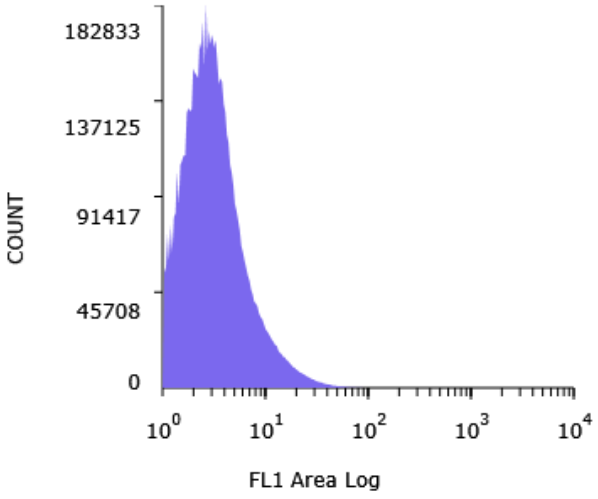

Figure 5. Fluorescence data of T98 cells after labelling with anti-CD133 antibody. Cells were incubated 10 minutes at 4°C in darkness before data acquisition using S3 sorter.

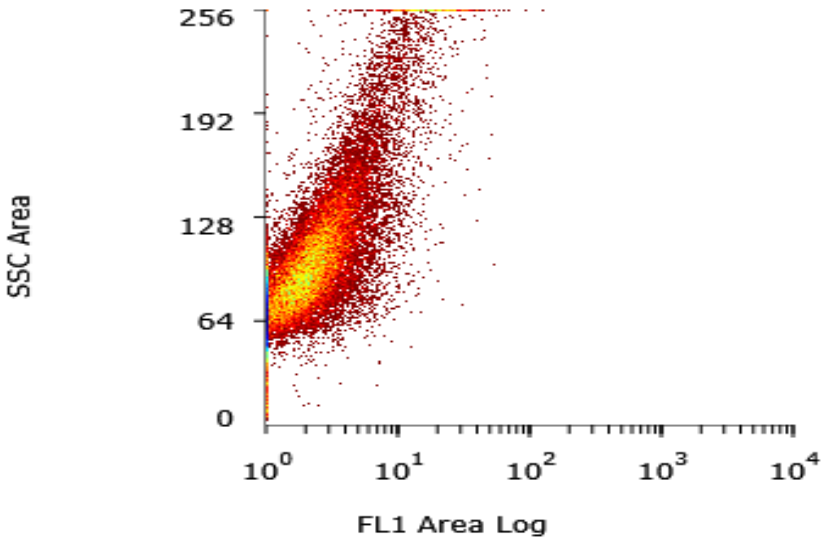

Figure 6. Scatterplot of T98 cells before labelling with anti-CD133 antibody.

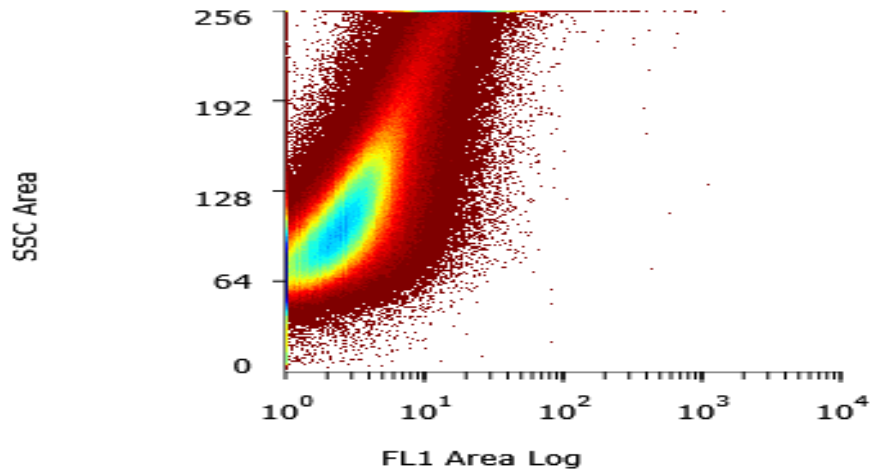

Figure 7. Scatterplot of T98 cells after labelling with anti-CD133 antibody.

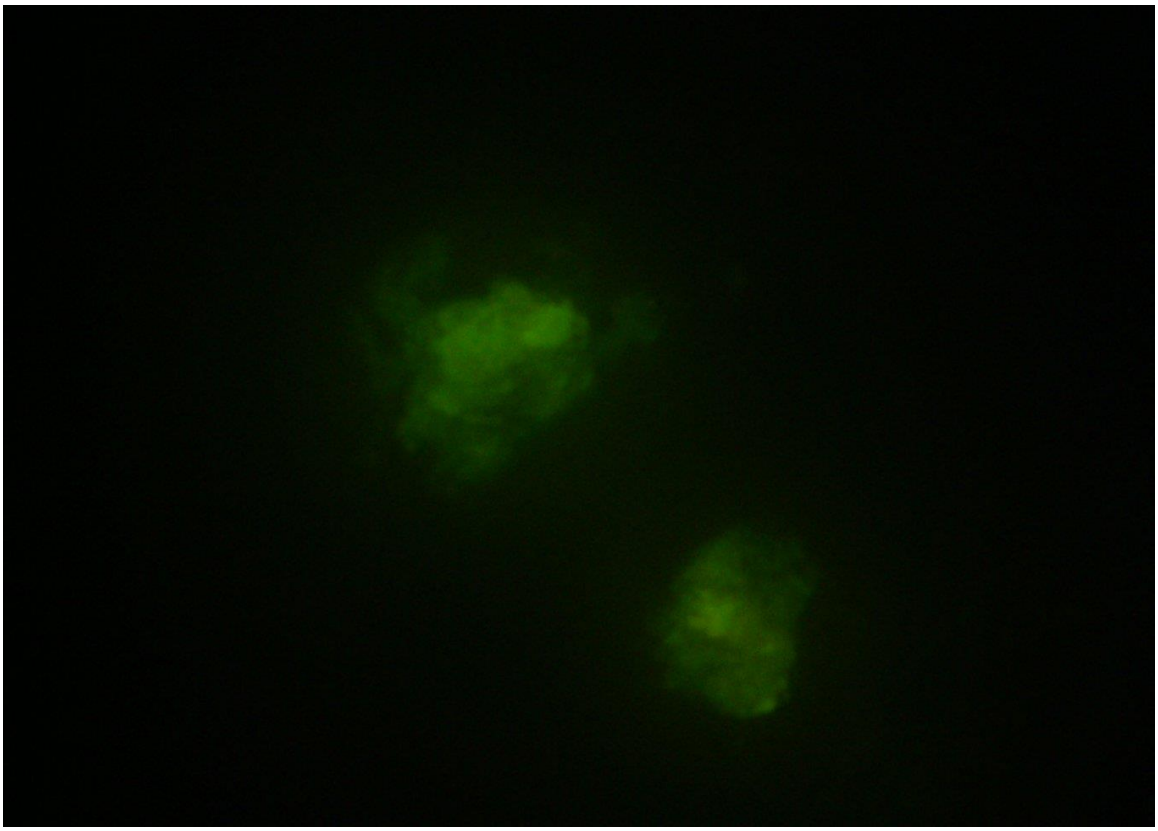

Figure 8. U87MG cells express surface CD147. Cells were labeled with FITC-conjugated anti-CD147 antibody (indicated by green in figure).

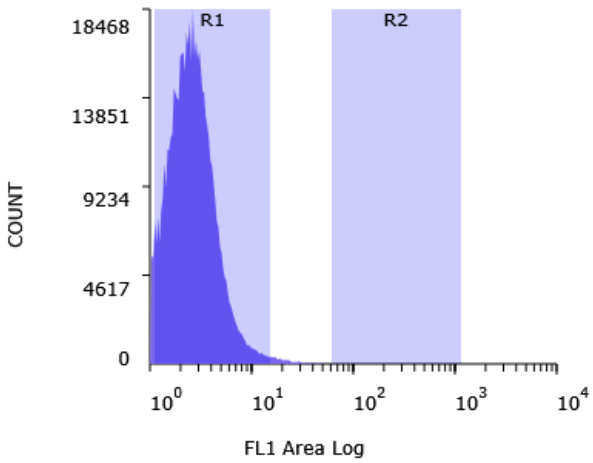

Figure 9. Histogram of U87MG cells before labelling with anti-CD147 antibody.

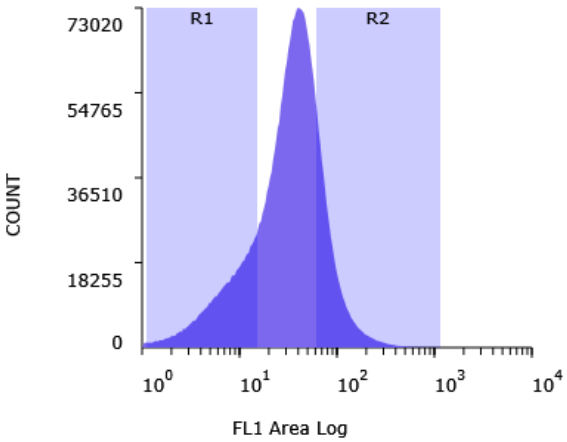

Figure 10. Fluorescent histogram of U87MG cells after labelling with anti-CD147 antibody. Blue bars represent sorting gates; 20% lowest-expressing-basigin (R1) and 20% highest-expressing-basigin (R2) cells were collected

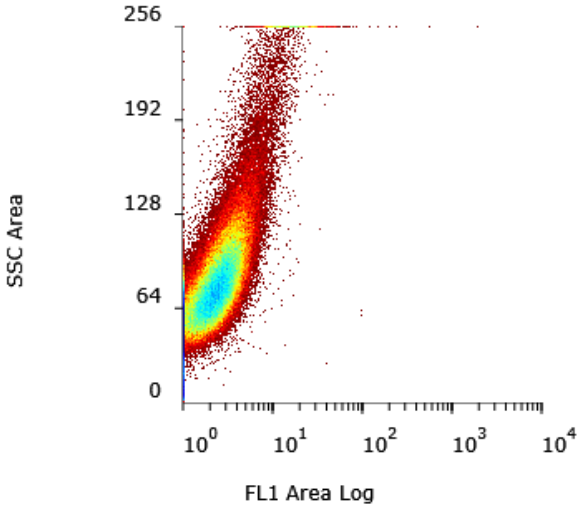

Figure 11. Scatterplot of U87MG cells before anti-CD147 antibody addition. Blue/green area indicates highest concentration of cells.

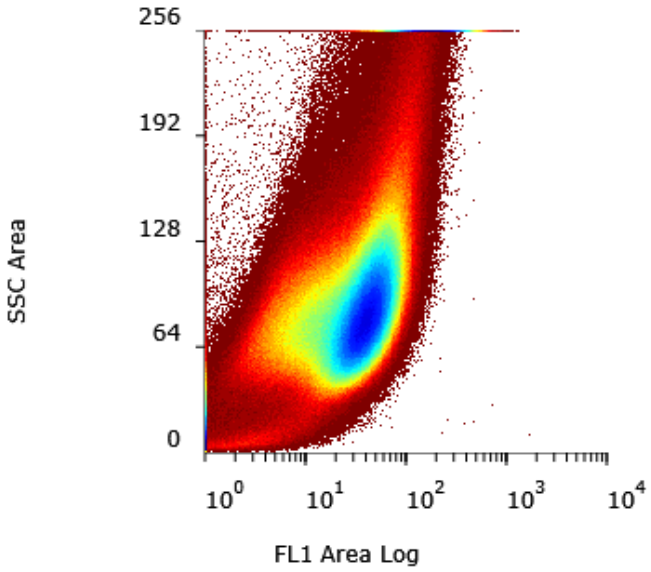

Figure 12. Scatterplot of U87MG cells after incubation with anti-CD147 antibody. Blue indicates presence of highest concentration of cells.

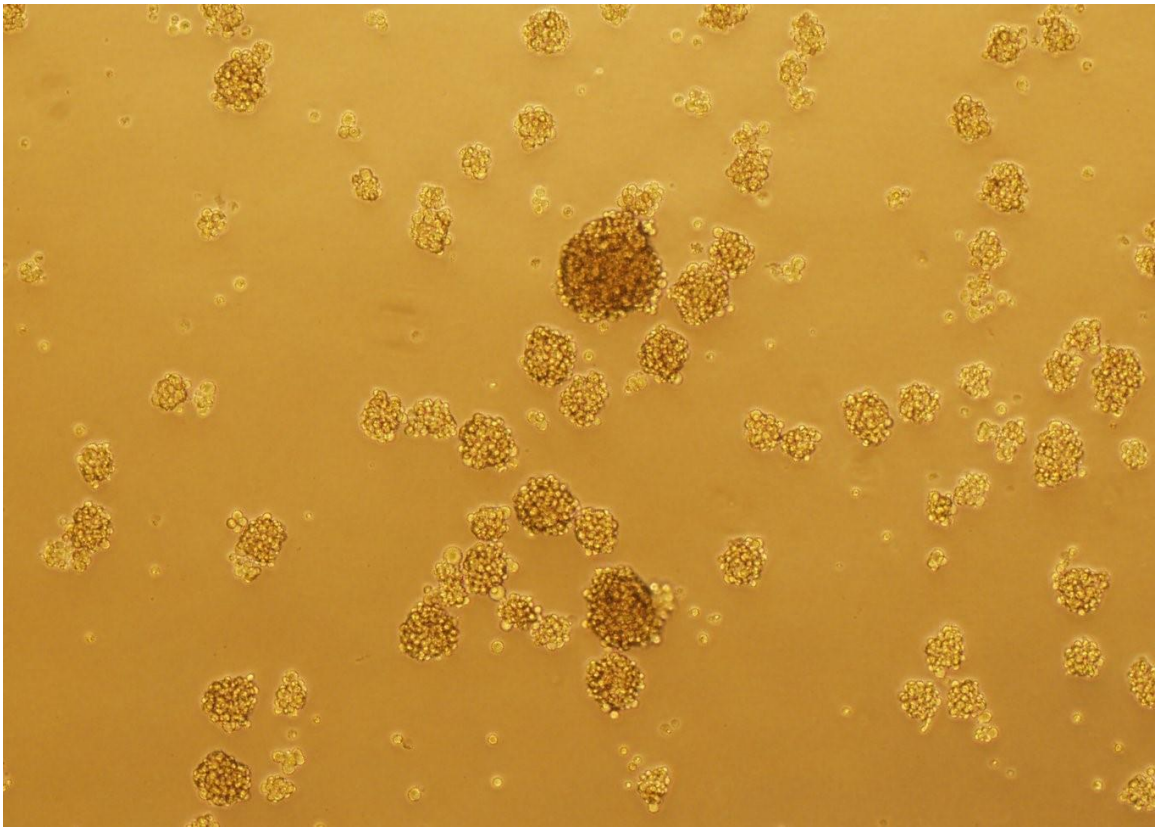

Figure 13. U87MG cells expressing high levels of CD147 form neurospheres in suspension culture. First group of cells incubated at 37^{0}C for 96 hours in hypoxic suspension culture. Image taken at 4X.

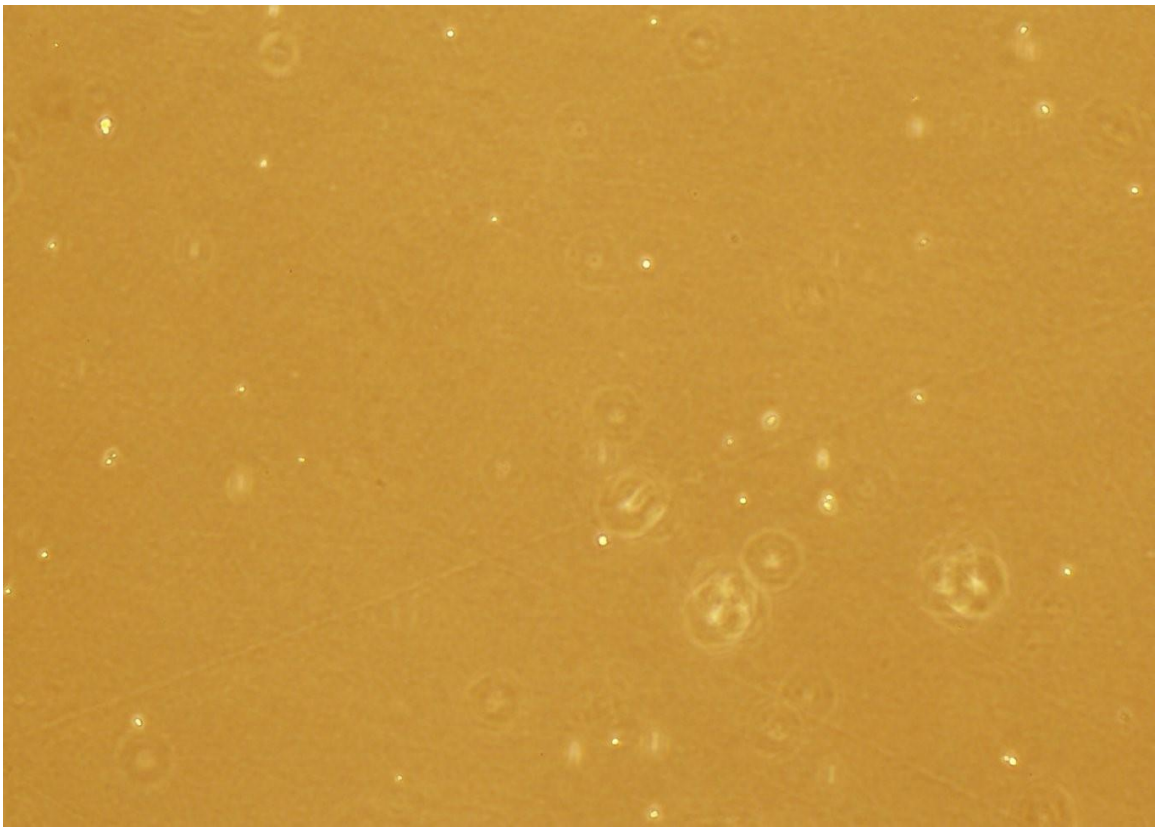

Figure 14. U87MG cells expressing low levels of CD147 do not form neurospheres in suspension culture. First group of cells incubated at 37°C for 96 hours in hypoxic suspension culture. Image taken at 4X.

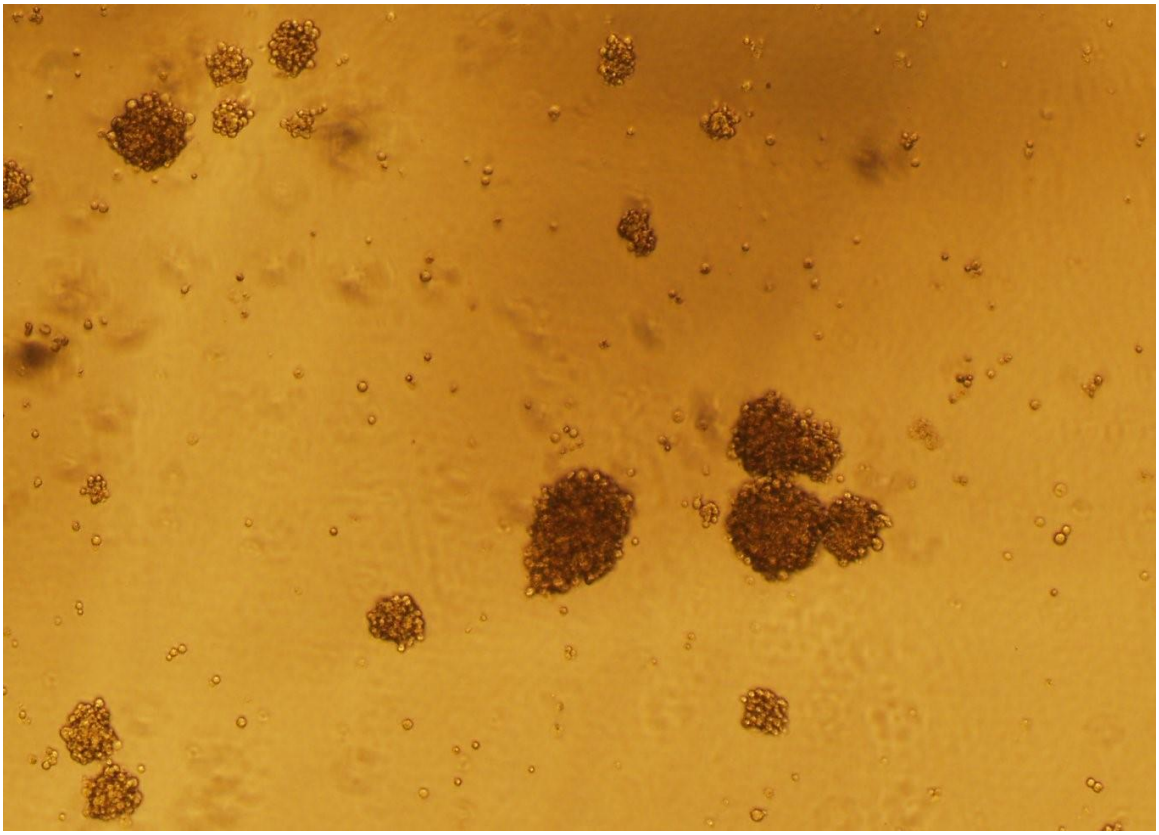

Figure 15. U87MG cells expressing high CD147 levels form neurospheres in suspension culture. Second group of cells incubated at 37°C after 96 hours in hypoxic suspension culture. Image at 4X.

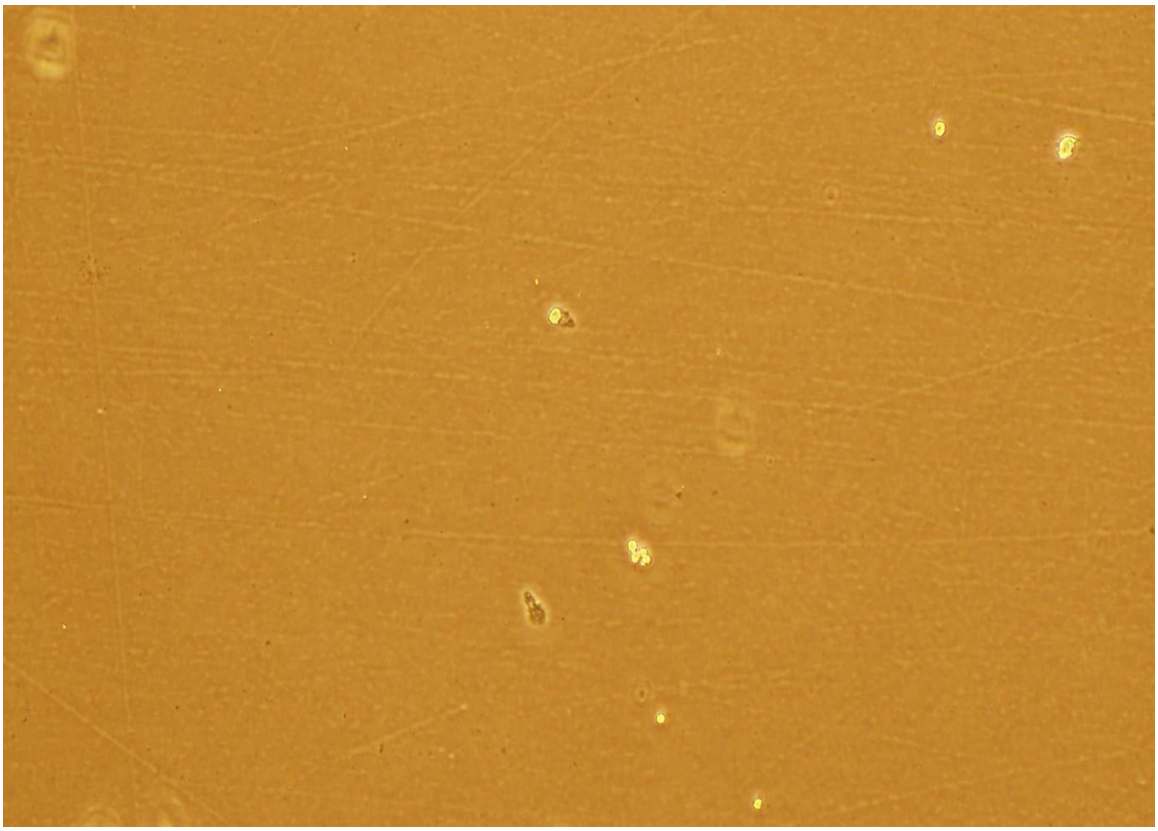

Figure 16. U87MG cells expressing low CD147 levels do not form neurospheres in suspension culture. Second group of cells incubated at 37ºC after 96 hours in hypoxic suspension culture. Image at 4X.

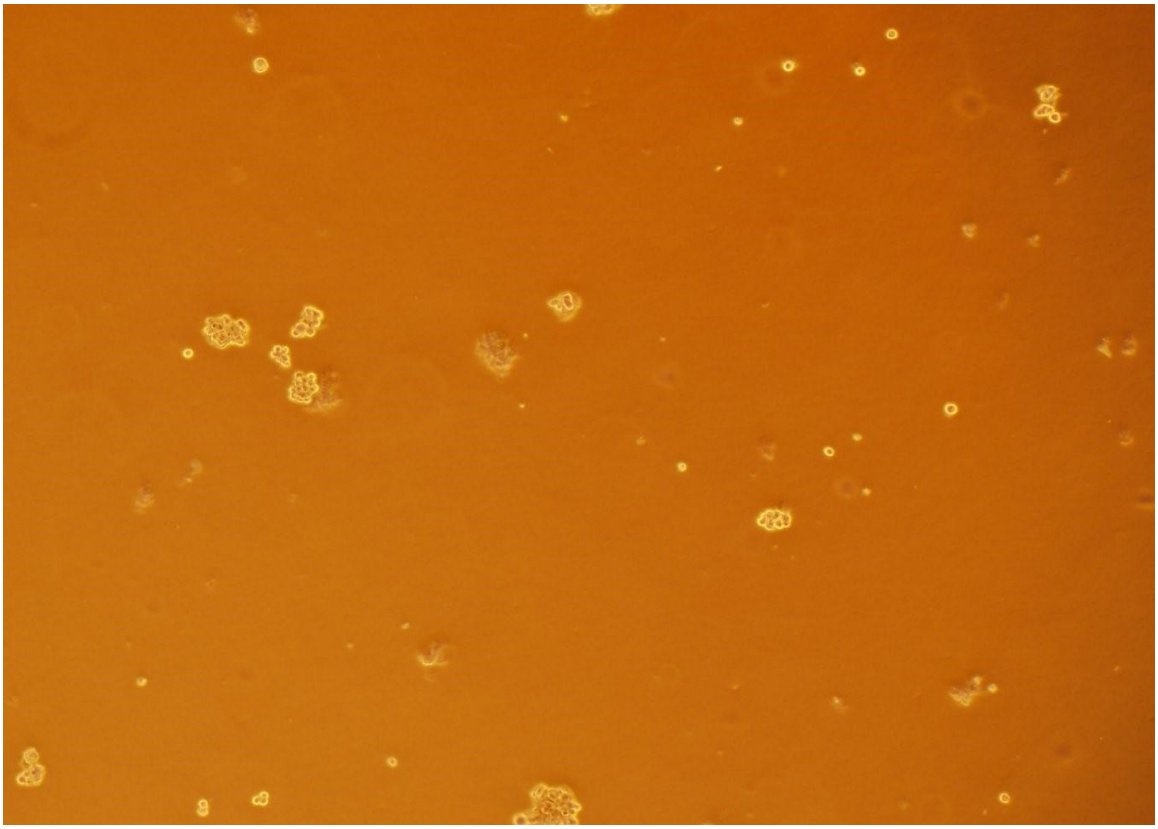

Figure 17. U87MG cells expressing high CD147 levels form neurospheres in suspension culture. Third group of cells incubated at 37°C after 96 hours in hypoxic suspension culture. Image at 4X.

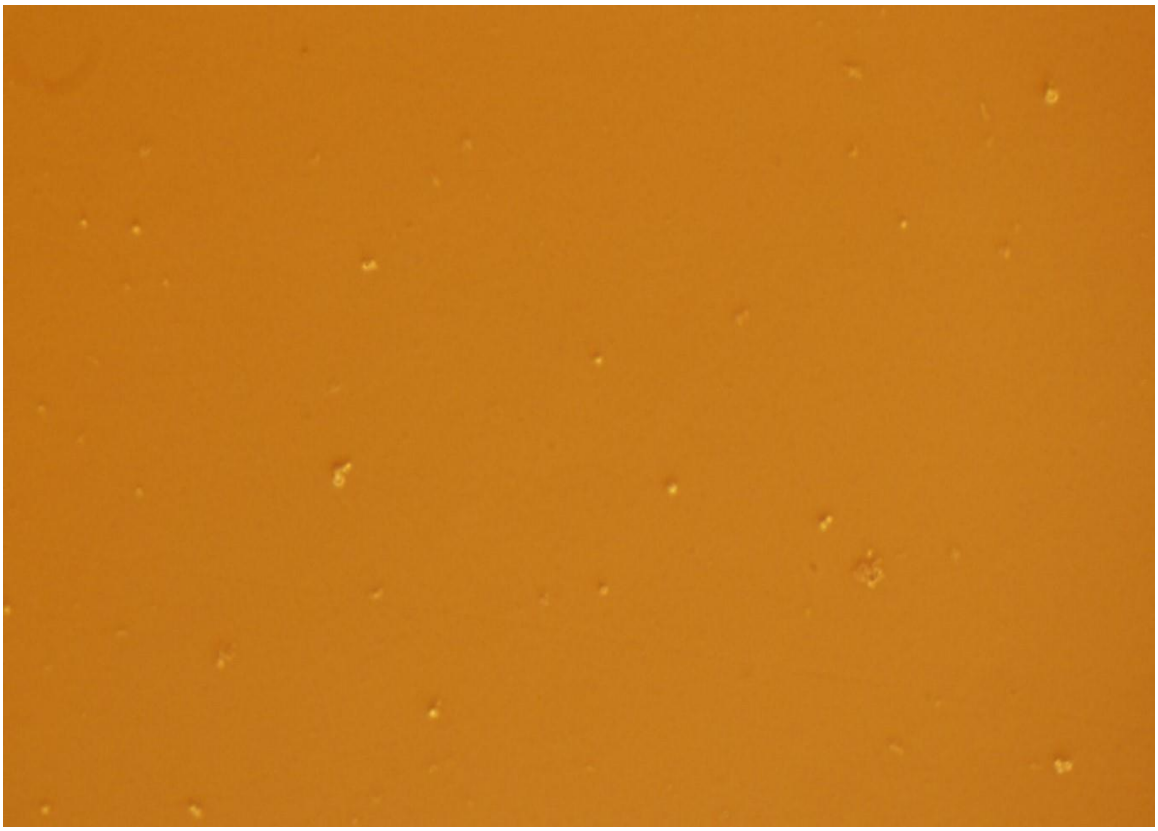

Figure 18. U87MG cells expressing low CD147 levels do not form neurospheres in suspension culture. Third group of cells incubated at 37ºC after 96 hours in hypoxic suspension culture. Image at 4X.

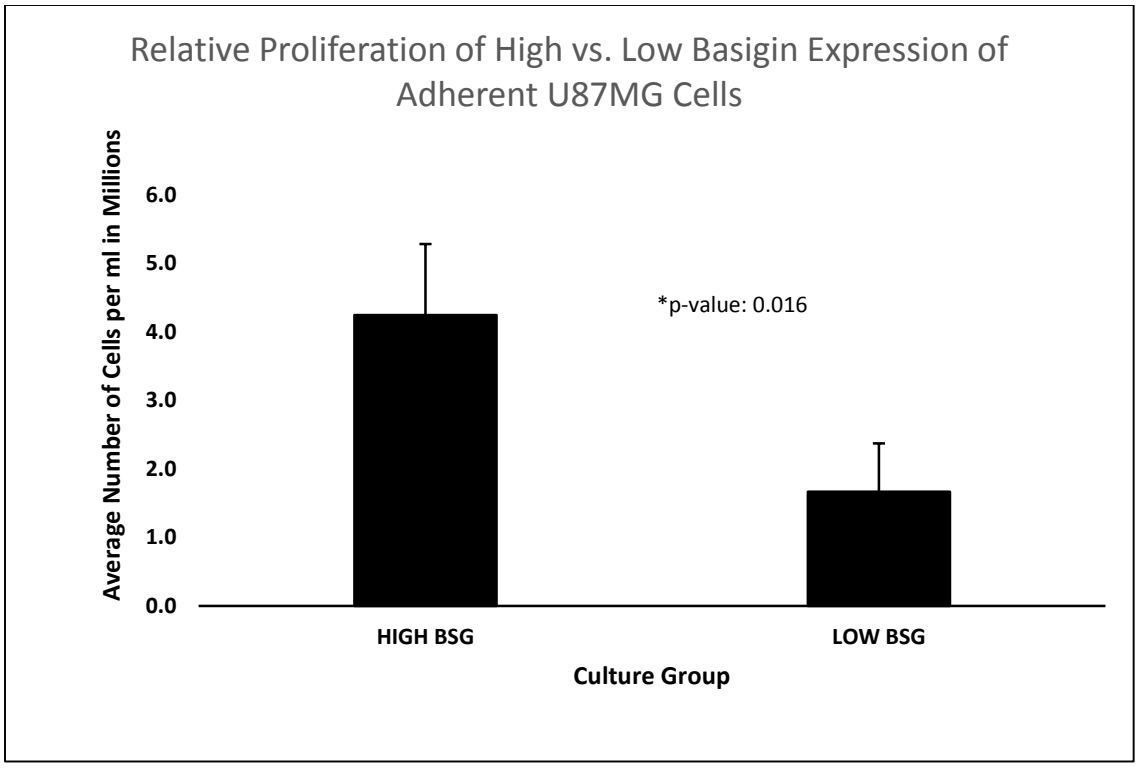

Figure 19. U87MG cells with increased CD147 expression are more proliferative. Comparison of relative proliferation levels of High CD147-expressing vs. Low CD147-expressing adherent U87MG cells. Cells were incubated 96 hours in hypoxia. Bars represent mean cell concentrations of three independent trials and standard error.

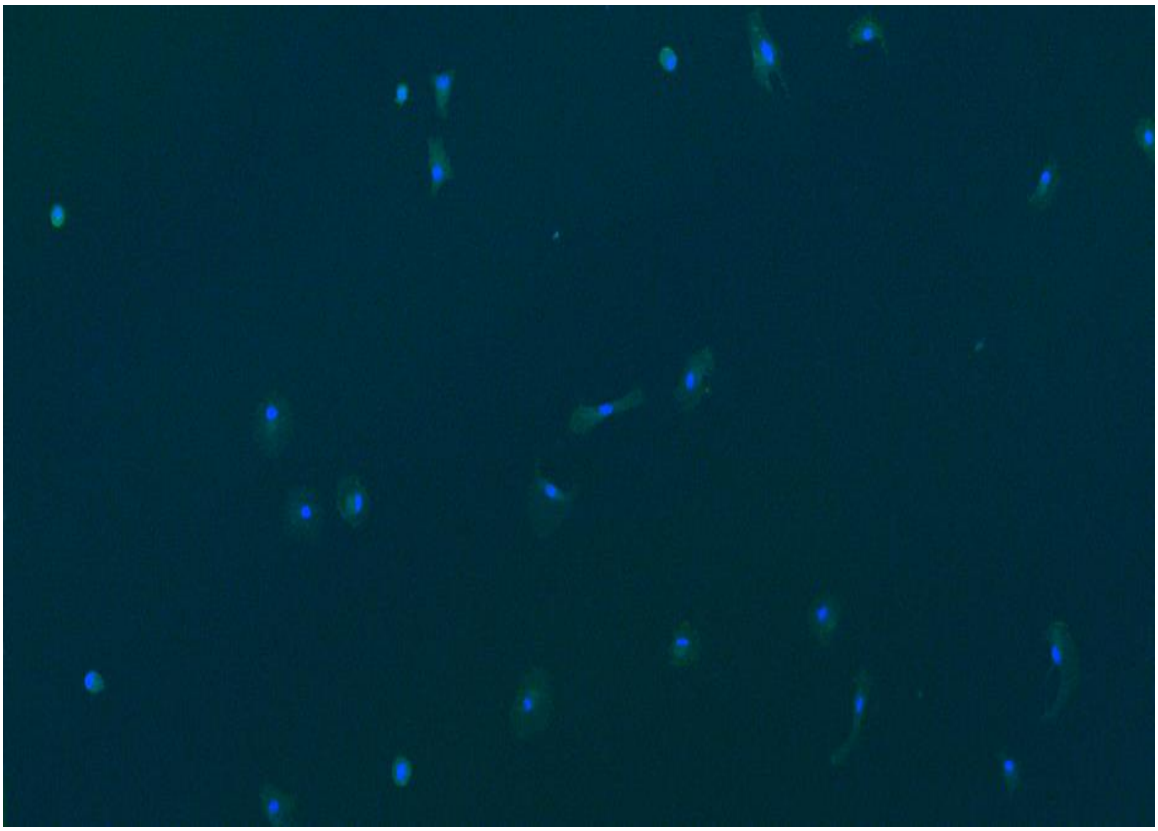

Figure 20. CD147 is expressed on U87MG cells. Laser Confocal Microscopy Image of U87MG cells expressing 20%-highest levels of CD147. Cells stained with DAPI (blue), labelled with anti-CD147 antibody with FITC conjugate (green). Image taken at 10X.

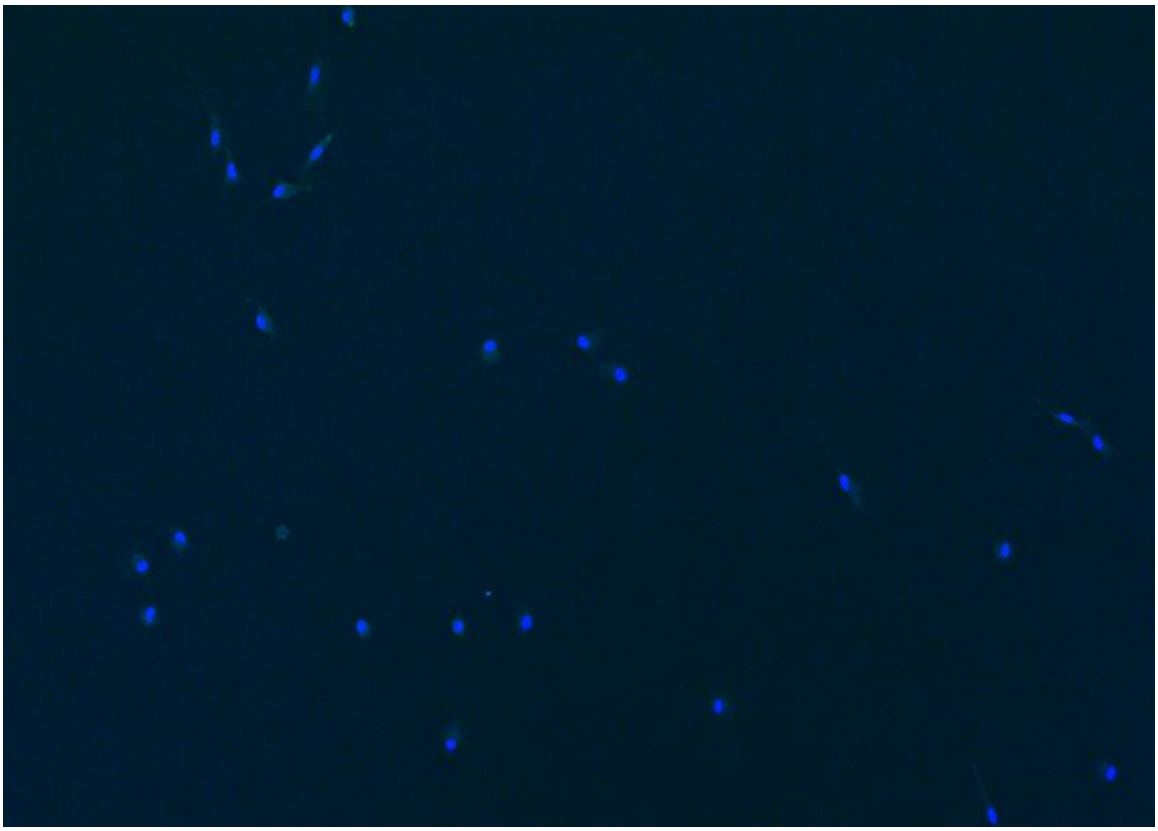

Figure 21. CD147 is absent on some U87MG cells. Laser Confocal Image of 20%-lowest-CD147-expressing U87MG cells stained with DAPI (blue) and anti-CD147 antibody conjugated with FITC (green). Image taken at 10X.

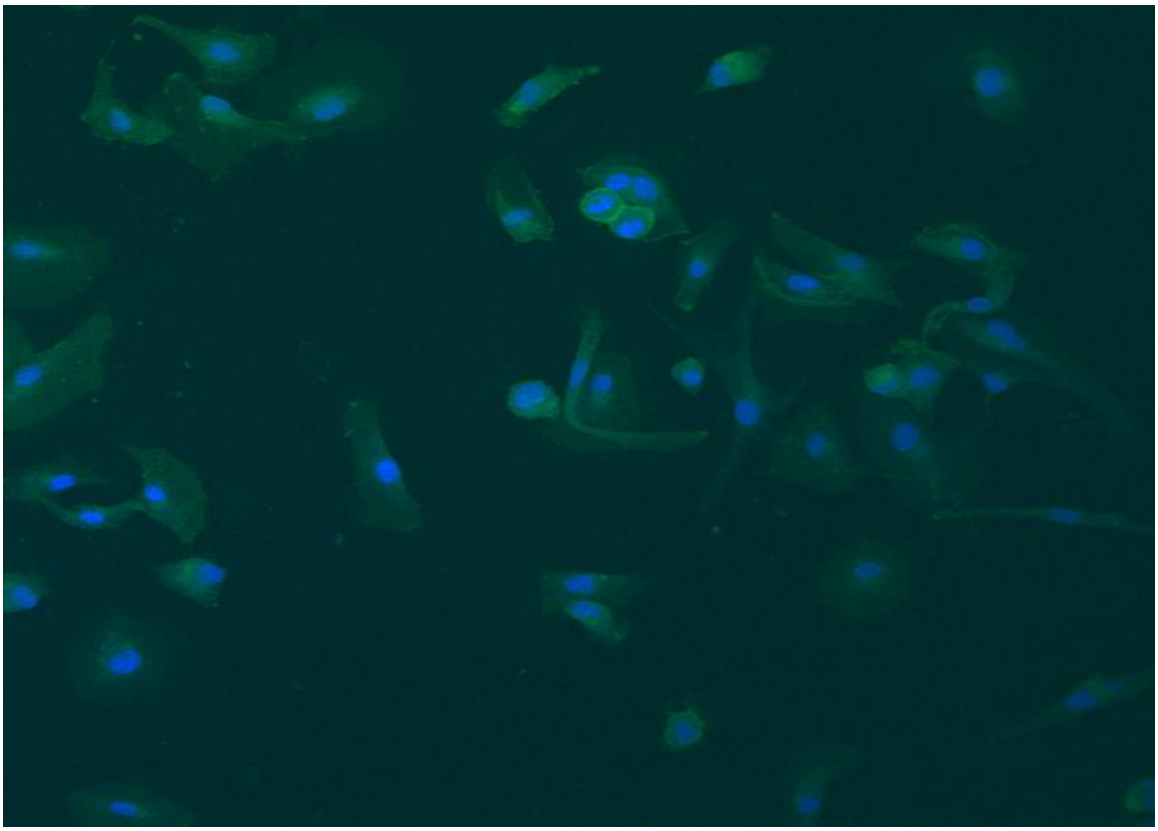

Figure 22. CD147 is expressed on U87MG cells. U87MG cells stained with DAPI (blue) and labelled with anti-CD147 antibody conjugated with FITC (green). Cells were among highest-1% CD147 expression. Image at 20X.

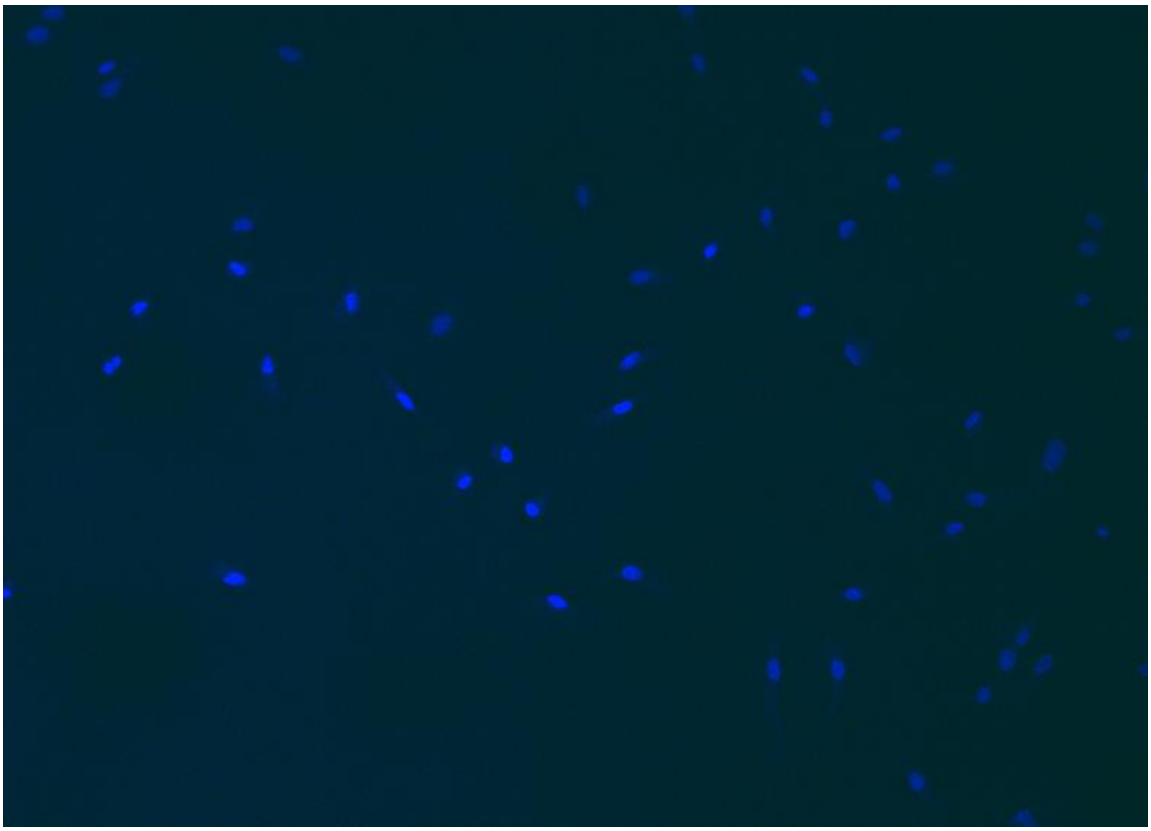

Figure 23. CD147 is not expressed on all U87MG cells. Laser confocal image shows lowest-1% of U87MG cells expressing CD147. Nuclei are DAPI stained (blue), cells labelled with anti-CD147 antibody conjugated with FITC. Image at 10X.

REFERENCES

1. Maher EA, Fumari FB, Bachoo RM, Rowitch DH, Louis DN et al. (2001) Malignant glioma:genetics and biology of a grave matter. Genes Dev 15: 1311-1333.
2. Vacas-Oleas A, de la Rosa J, Garcia-Lopez R, Vera-Cano B, Gallo-Oller G, et al. (2013) In vitro tumorigenicity and stemness characterization of the U87MG glioblastoma cell line based on the CD133 cancer stem cell marker. 2:609 doi:10.4172/scientificreports.609.
3. Singh A, Settleman J (2010) EMT, cancer stem cells and drug resistance: an emerging axis of evil in the war on cancer. Oncogene 29:4741-4751.
4. Beier D, Hau P, Proescholdt M, Lohmeier A, et al. CD133(+) and CD133(-) glioblastoma-derived cancer stem cells show differential growth characteristics and molecular profiles. Cancer Res. 2007 May 1;6 (9):4010-5.
5. Kievit FM, Florczyk SJ, Leung MC, Wang K et al. (2014) Proliferation and enrichment of CD133+ glioblastoma cancer stem cells on 3D chitosan-alginate scaffolds. Biomaterials 35(2014)9137-9143.
6. Thiery JP, Acloque H, Huang RY, Nieto MA. Epithelial-mesenchymal transitions in development and disease. Cell 2009;139:871-890.
7. Miraglia S, Godfrey W, Yin AH, Atkins K, Warnke R et al. A novel 5-transmembrane hematopoietic stem cell antigen: isolation, characterization, and molecular cloning. Blood 1997;90:5013-21.
8. Irollo E and Pirozzi G. CD133: to be or not to be, is this the real question? Am J Transl Res 2013;5(6):563-581.
9. Singh SK, Hawkins C, Clarke ID, Squire JA, Bayani J, Hide T, Henkelman RM, Cusimano MD, Dirks PB. Identification of human brain tumor initiating cells. Nature 2004;432:396-401.
10. Wang J, Sakariassen PO, Tsinkalovsky O, Immervoll H, Boe SO, Svendsen A, Prestegarden L et al. CD133 negative glioma cells form tumors in nude rats and give rise to CD133 positive cells. Int J Cancer 2008;122;761-768.
11. Kemper K, Sprick MR, de Bree M, Scopelliti A, Vermuelen L, et al. The AC133 epitope, but not the CD133 protein, is lost upon cancer stem cell differentiation. Cancer Res 2010;70:719-29.
12. Bidlingmaier S, Zhu X, Liu B. The utility and limitations of glycosylated human CD133 epitopes in defining cancer stem cells. J Mol Med (Berl) 2008; 86:1025-1032.
13. Donovan LK, Potter NE, Warr T, Pilkington GJ. A prominin-1-rich pediatric glioblastoma: biologic behavior is determined by oxygen tension-modulated CD133 expression but not accompanied by underlying molecular profiles. Trans Oncol 2012;5:141-54.
14. Tabu K, Sasai K, Kimura T, Wang L, Aoyanagi E, Kohsaka S, Tanino M, Nishihara H, Tanaka S. Promoter hypomethylation regulates CD133 expression in human gliomas. Cell Res 2008;18:1037-1046.

15. He et al. GSC markers and MGMT in glioma radioresistance. Oncol Rep 2011; 26:1305-1313.
16. Cheng JX, Liv BL and Zhang X. How powerful is CD133 as a cancer stem cell marker in brain tumors? Cancer Treat Rev 2009. 35:403-408.
17. Bredel M and Zentner J. Brain-tumour drug resistance: the bare essentials. Lancet Oncol 2002. 3:397-406.
18. Rivera AL, Pelloski CE, Gilbert MR et al. MGMT promoter methylation is predictive of response to radiotherapy and prognostic in the absence of adjuvant alkylating chemotherapy for glioblastoma. Neuro Oncol 2010. 12:116-121.
19. Chinot OL, Barrie M, Fuentes S et al. Correlation between O6-methylguanine-DNA-methyltransferase and survival in inoperable newly diagnosed glioblastoma patients treated with neoadjuvant temozolomide. J Clin Oncol 2007;25:1470-1475.
20. Kanekura T, Chen X, Kanzaki T. Basigin (CD147) is expressed on melanoma cells and induces tumor cell invasion by stimulating production of matrix metalloproteinases by fibroblasts. Int J Cancer 2002 Jun 1;99(4):520-528.
21. Mathupala SP, Colen CB, Parajuli P, Sloan AE. Lactate and malignant tumors: a therapeutic target at the end stage of glycolysis (Review). J Bioenerg Biomembr. **39**(1):73–77.
22. Belton et al. Basigin-2 is a cell-surface receptor for soluble basigin ligand. J Biol Chem 2008 283(26)17805-17814.
23. Wu et al. Full-length soluble CD147 promotes MMP-2 expression and is a potential serological marker in detection of hepatocellular carcinoma. J Trans Med 2014 12:190.
24. Xiong L, Edwards CK, Zhou L. The biological function and clinical utilization of CD147 in human diseases: a review of the current scientific literature. Int J Mol Sci 2014,15,17411-17441.
25. Gabison et al. Differential expression of extracellular matrix metalloproteinase inducer (CD147) in normal and ulcerated corneas: Role in epithelio-stromal interactions and matrix metalloproteinase induction. Am J Pathol 2005, 166, 209-219.
26. Tsai et al. EMMPRIN expression positively correlates with WHO grades of astrocytomas and meningiomas. J Neurooncol 2013, 114:281-290.
27. Pistollato, Abbadi, Rampazzo, et al. Intratumoral hypoxic gradient drives stem cells distribution and MGMT expression in glioblastoma. Stem Cells 2010; 28:851-862.
28. Hegi ME, Diserens AC, Gorlia T et al. MGMT gene silencing and benefit from temozolomide in glioblastoma. N Engl J Med 2005;352:997-1003.
29. Bar et al. Hypoxia increases the expression of stem-cell markers and promotes clonogenicity in glioblastoma neurospheres. Am J Pathol 2010 Sep;177(3): 1491-1502.
30. Heddleston JM, Li Z, McLendon RE et al. The hypoxic microenvironment maintains glioblastoma stem cells and promotes reprogramming towards a cancer stem cell phenotype. Cell Cycle 2009; 8:3274-3284.

31. A. Filatova, et al. The cancer stem cell niche(s): The crosstalk between glioma stem cells and their microenvironment. Biochim Biophys Acta 2012, http://dx.doi.org/10.1016/j.bbagen.2012.10.008.
32. Hjelmeland AB, Wu Q, et al. Acidic stress promotes a glioma stem cell phenotype. Cell Death Differ. 2011;18 829-840.
33. Brescia P et al. CD133 is essential for glioblastoma stem cell maintenance. Stem Cells 2013 May;(31)5:857-69.
34. Rahman et al. Neurosphere and adherent culture conditions are equivalent for malignant glioma cell lines. Anat Cell Biol 2015;48:25-35.
35. Xia et al. Loss of brain-enriched miR-124 enhances the stem-like traits and invasiveness of glioma cells. Jour Biol Chem 2012 (published online)
36. Hong X, Chedid K, Kalkanis S. Glioblastoma cell line-derived spheres in serum-containing medium versus serum-free medium: A comparison of cancer stem cell properties. Int Jour Oncol 2012 41:1693-1700.
37. Ulasov IV, Nandi S, Dey M, Sonabend AM, Lesniak MS. Inhibition of Sonic Hedgehog and Notch pathways enhances sensitivity of CD133(+) glioma stem cells to temozolomide therapy. Mol Med 2011 17:103-112.
38. Barrangou R, Fremaux C, Deveau H et al. CRISPR provides acquired resistance against viruses in prokaryotes. Science 2007 315(5819):1709-1712.
39. Mali P, Yang L, Esvelt KM, Aach J, Guell M, Dicarlo JE, Norville JE, Church GM. RNA-guided human genome engineering via Cas9. Science 2013 339(6121):823-826.